Magnetization of 0-29 Ma ocean crust on the Mid-Atlantic Ridge, 25°30' to 27°10'N

Maurice A. Tivey and Brian E. Tucholke

Department of Geology and Geophysics, Woods Hole Oceanographic Institution, Woods Hole, Massachusetts

Abstract. A sea-surface magnetic survey over the west flank of the Mid-Atlantic Ridge from 0 to 29 Ma crust encompasses several spreading segments and documents the evolution of crustal magnetization in slowly accreted crust. We find that magnetization decays rapidly within the first few million years, although the filtering effect of water depth on the sea-surface data and the slow spreading rate (<13 km/m.y.) preclude us from resolving this decay rate. A distinctly asymmetric, along-axis pattern of crustal magnetization is rapidly attenuated off-axis, suggesting that magnetization dominated by extrusive lavas on-axis is reduced off-axis to a background value. Off-axis, we find a statistically significant correlation between crustal magnetization and apparent crustal thickness with thin crust tending to be more positively magnetized than thicker crust, indicative of induced magnetization in thin inside corner (IC) crust. In general, we find that off-axis segment ends show an induced magnetization component regardless of polarity and that IC segment ends tend to have slightly more induced component compared with outside corner (OC) segment ends, possibly due to serpentinized uppermost mantle at IC ends. We find that remanent magnetization is also reduced at segment ends, but there is no correlation with inside or outside corner crust, even though they have very different crustal thicknesses. This indicates that remanent magnetization off-axis is independent of crustal thickness, bulk composition, and the presence or absence of extrusives. Remanence reduction at segment ends is thought to be primarily due to alteration of lower crust in OC crust and a combination of crustal thinning and alteration in IC crust. From all these observations, we infer that the remanent magnetization of extrusive crust is strongly attenuated off-axis, and that magnetization of the lower crust may be the dominant source for off-axis magnetic anomalies.

1. Introduction

A key tenet of plate tectonics is that the marine magnetic anomaly pattern observed over the ocean basins arises because seafloor spreading records the episodic polarity reversals of the geomagnetic field [*Vine and Matthews*, 1963]. For fast-spreading ridges, the nearly steady state crustal accretion process and the "constant" spatial and temporal recording of the ambient magnetic field creates strongly lineated and highly correlatable magnetic anomalies that are well resolved [e.g., *Macdonald*, 1982]. In contrast, slow-spreading ridges are typified by spatially and temporally variable crustal accretion and tectonism that give rise to poorly developed and discontinuous magnetic anomalies [e.g., *Vogt*, 1986]. Recent investigations of the slow-spreading Mid-Atlantic Ridge (MAR) have significantly improved our understanding of the complex, three-dimensional crustal architecture of slowly accreted crust [e.g., *Macdonald*, 1986; *Lin et al.*, 1990; *Sinton and Detrick*, 1992; *Tucholke and Lin*, 1994; *Cannat et al.*, 1995]. Along the axis of the Mid-Atlantic Ridge, segment midpoints tend to be systematically shallower and exhibit mantle Bouguer gravity lows (bull's-eyes) at their midpoints [e.g., *Kuo and Forsyth*, 1988; *Lin et al.*, 1990]. These observations suggest that ocean crust is thicker at segment centers than at segment ends, which is consistent with available seismic results [*Sinha and Louden*, 1983; *Tolstoy et al.*, 1993].

Crustal structure is further complicated by strong cross-rift asymmetry near segment ends. Inside corner (IC) crust, formed in the zone bounded by the spreading axis and active offset, typically has shallow and irregular topography, exposures of plutonic and ultramafic rocks, and elevated residual mantle Bouguer gravity anomaly (RMBA) that suggests thin crust [*Tucholke and Lin*, 1994; *Tucholke et al.*, 1997]. Conjugate outside corner (OC) crust, formed on the opposite side of the ridge axis, is deeper, exhibits regular ridge-parallel abyssal hills of basaltic composition, and has reduced RMBA. IC crust is thought to be tectonically thinned, forming the footwalls of low-angle detachment faults that dip toward the ridge axis; conjugate OC crust forms the hanging walls and contains "normal" crust with the basalt and dike carapace intact [*Dick et al.*, 1981; *Karson*, 1990; *Tucholke and Lin*, 1994]. These complex patterns of crustal accretion and tectonic dismemberment near the spreading axis create spatially heterogeneous crustal sections off-axis, and they have important implications for the initial recording of the geomagnetic signal, the long-term preservation of crustal magnetization, and the nature of the marine magnetic anomaly source.

2. Crustal Magnetization at Slow-Spreading Ridges

Recent magnetic studies of slow-spreading ridges have focused on along-axis variability in crustal magnetization and have defined a moderately systematic pattern. Crustal magnetization is found to be weakest at segment midpoints where crust is thought to be thickest, while apparently thinner crust at segment ends has relatively higher magnetization [*Carbotte et al.*, 1991; *Grindlay*

et al., 1992; *Weiland et al.*, 1996; *Hussenoeder et al.*, 1996; *Pariso et al.*, 1996]. Several hypotheses have been proposed to explain this variation. For the South Atlantic, *Grindlay et al.* [1992] proposed that shallow Curie isotherms at segment centers thin the source layer along the ridge axis; this is a thermal effect that should disappear with age. However, in the North Atlantic south of Kane Fracture Zone, *Pockalny et al.* [1995] found segment-scale, along-axis variations in magnetization that continue off-axis, thus invalidating the Curie isotherm hypothesis. Another hypothesis emphasizes the relationship between FeO content and magnetization [*Vogt and Johnson*, 1973]. Although magnetization intensity is a function of grain size, alteration state, and other variables, it has been convincingly demonstrated that increased FeO content correlates with stronger magnetization on fast-spreading ridges such as the East Pacific Rise (EPR) [e.g., *Sempéré et al.*, 1984; *Sempéré*, 1991]. This relationship is difficult to observe on the slow-spreading MAR because of large scatter in data. *Weiland et al.* [1996], however, correlated rock magnetism with magnetic anomaly amplitude in the South Atlantic and concluded that FeTi enrichment of basalts toward the ends of segments could provide sufficient magnetization contrast to produce the observed variations.

Complexities in crustal magnetization related to on-axis accretion are further compounded by effects of tectonism associated with off-axis transport in slow-spreading environments and by magnetization decay with age. Few detailed studies have looked off-axis to investigate these effects. *Pockalny et al.* [1995] found that off-axis crust near discontinuities on the MAR south of Kane Fracture Zone is marked by generally positive magnetization, regardless of polarity, and they attributed this to serpentinization. They did not investigate the relationship between crustal magnetization and IC versus OC tectonic setting, partly because of the complex segmentation history and limited age extent of their study area (< 10 m.y.). In a study of the MAR between 28° and 30°N, *Pariso et al.* [1996] also found relatively positive crustal magnetization along discontinuities, and they suggested that this was caused by induced magnetization in serpentinized mantle; again, no attempt was made to look at IC/OC differences.

Decay of magnetization with age is also an important aspect of crustal magnetization. Studies based on Deep Sea Drilling Project and Ocean Drilling Program samples have found that magnetization in the extrusive crust decreases over a 20 m.y. period, primarily because of low-temperature oxidation of magnetite [*Irving*, 1970; *Vogt*, 1986; *Bleil and Peterson*, 1983; *Johnson and Pariso*, 1993]. Magnetic anomalies offer a more continuous sampling of crustal magnetization than borehole or seafloor samples, and they represent the contribution of the entire magnetic source layer rather than just the extrusive crust. Magnetic anomaly studies separate magnetization decay into initial rapid decay, superimposed on long-term decay. *Wittpenn et al.* [1990] analyzed South Atlantic magnetic anomaly inversions and found an initial rapid decay in amplitude over the first 5 m.y., followed by a slower, long-term decay over 18 m.y. Recent North Atlantic studies also suggest rapid decay over the first 5 m.y. [*Pockalny et al.*, 1995; *Pariso et al.*, 1996]; however, magnetic anomaly C5n (9.592-10.834 Ma [*Cande and Kent*, 1995]) does not fit the decay curve, which led *Pariso et al.* to invoke a two-layer crustal model to enhance magnetization at chron C5n. Unfortunately, these studies reached only to 10 Ma crust, so they do not adequately sample the long-term signal of magnetization decay.

Magnetization may decay even more quickly than in the 5 m.y. time frame noted above. Early deep-tow magnetic studies in the

French-American Mid-Ocean Undersea Study (FAMOUS) area at 37°N on the MAR found a magnetization decay time (i.e., decay to 1/e of initial value) of only 500,000 years [*Macdonald*, 1977], consistent with direct measurements of rock samples from the same region [*Johnson and Atwater*, 1977]. Recent deep-tow magnetic profiles just north of Kane Fracture Zone suggest a faster decay time of 150,000 years [*Hussenoeder et al.*, 1996]. Even shorter decay times have been suggested for the fast-spreading EPR (e.g., 20,000 years [*Gee and Kent*, 1994]), and results from zero-age lavas of the Juan de Fuca Ridge suggest that initial decay time might be less [*Johnson and Tivey*, 1995; *Tivey and Johnson*, 1995]. The intrinsic decay rate of magnetic minerals caused by low-temperature alteration is unlikely to vary as widely as these rates suggest; rather, the wide range of apparent decay times probably reflects a real decay caused by alteration, convolved with spatial averaging of the zone of crustal emplacement. For example, slow-spreading ridges generally have a wider zone of crustal accretion than fast-spreading ridges [*Macdonald et al.*, 1988], which may account for their greater apparent decay times.

In this study, our long (29 m.y.) and detailed magnetic record allows us to fully evaluate the effects of crustal aging on magnetization, i.e., over a time span which encompasses the 20 m.y. range of magnetization decay studied by *Johnson and Pariso* [1993] as well as the 5 m.y. decay time emphasized by other studies. We also investigate the relations between the sea-surface magnetic anomaly signal and intrasegment tectonic setting. From this analysis, we speculate about the source of off-axis magnetic anomalies and propose mechanisms to explain the observed along-isochron variations in magnetization.

3. Magnetic Data Collection and Analysis

Magnetic data used in this study were collected as part of the Office of Naval Research (ONR) Acoustic Reverberation Special Research Program (ARSRP) conducted in 1992 on the west flank of the MAR (Figure 1). The primary goal of the ARSRP was to understand acoustic reverberation from the seafloor through detailed seafloor mapping over a wide range of scales using several different geophysical techniques. Sea-surface surveys acquired Hydrosweep multibeam bathymetry, Hawaii MR1 long-range sidescan sonar, single-channel seismic reflection, and magnetic and gravity data in a 200 km-wide corridor that extended 400 km westward from the MAR axis to ~29 Ma crust (Figure 1).

Total magnetic field data were obtained using a towed proton precession magnetometer during R/V Ewing cruise EW9208 (Figure 2). These data were corrected for the regional geomagnetic field for 1992 by interpolation between the 1990 Definitive Geomagnetic Reference Field (DGRF) and the 1995 International Geomagnetic Reference Field (IGRF) model [*International Association of Geomagnetism and Aeronomy (IAGA)*, 1996]. The EW9208 data were then combined with magnetic field data from the MARNOK survey [*Purdy et al.*, 1990; *Sempéré et al.*, 1993] collected over the MAR ridge axis in 1989 and 1990; the MARNOK data were reduced to anomaly by interpolation between the 1985 and 1990 DGRF field models. The combined data were then embedded within a larger grid of magnetic data (~5 km grid resolution) from a Canadian North Atlantic magnetic database compilation [*McNab et al.*, 1995] between Atlantis and Kane Fracture Zones. An offset of 98 nT was added to the MARNOK and EW9208 data to fit the Canadian database. These
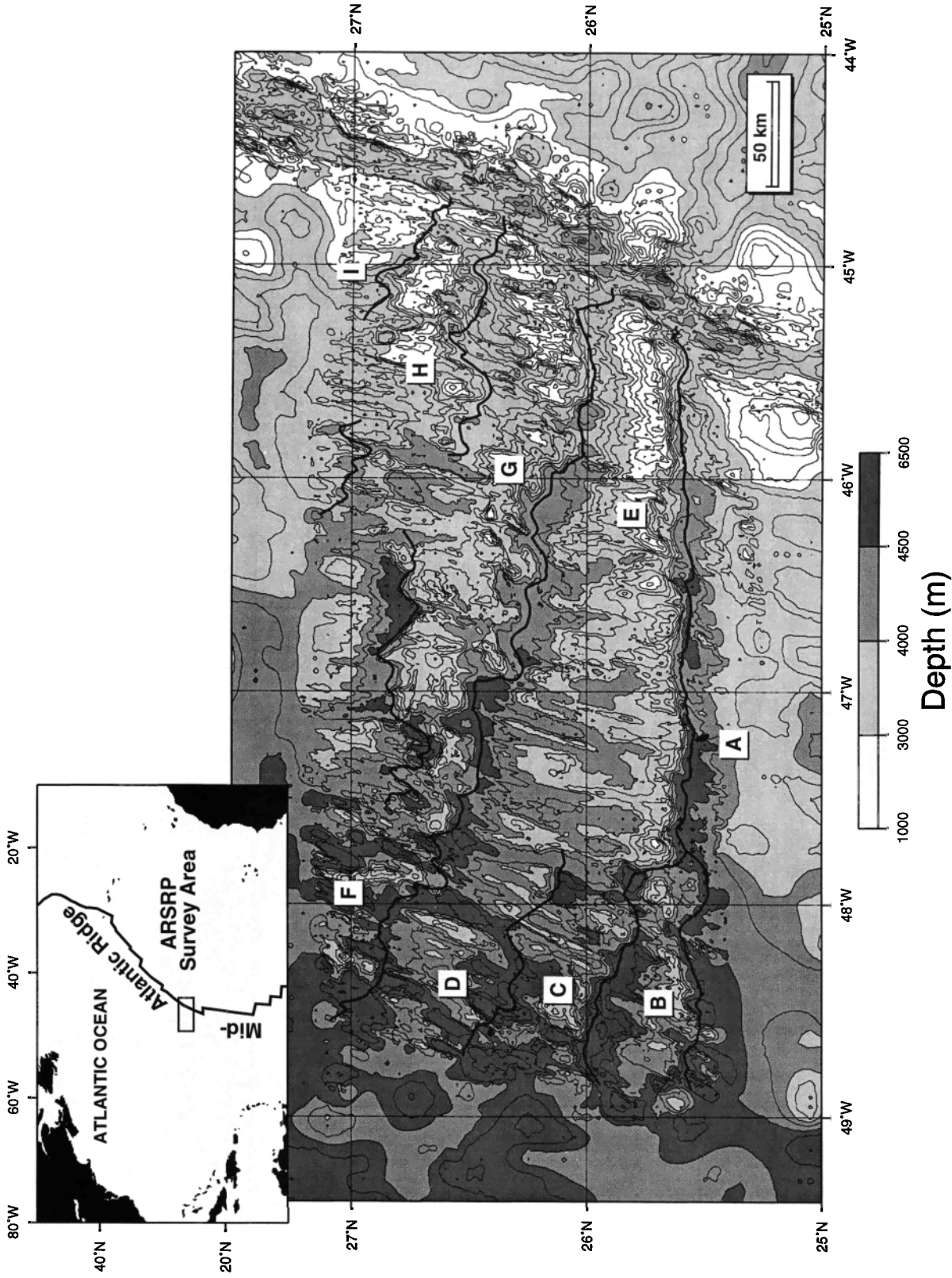
Figure 1. Multibeam bathymetry in the Acoustic Reverberation Special Research Program (ARSRP) study area on the west flank of the Mid-Atlantic Ridge. Contour interval is 250 m. Discontinuities between spreading segments are shown by bold lines and letters refer to segments discussed in the text. Low-resolution bathymetry data at the perimeter of the figure are from the Canadian database compilation of *McNab et al.* [1995]. Inset map shows study location.
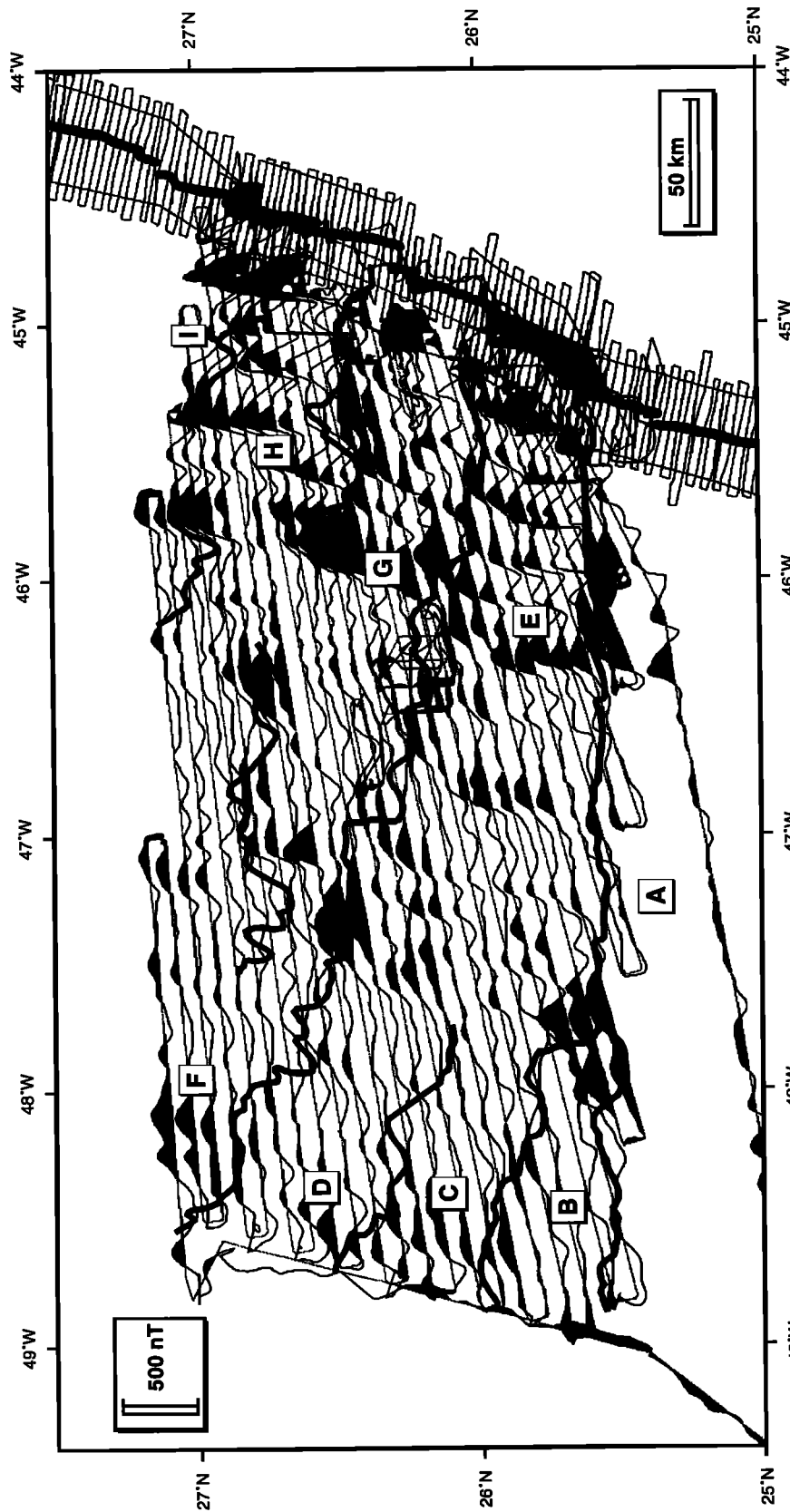
Figure 2. Trackline map of EW9208 (ridge flank) survey and MARNOK survey (ridge axis) [*Purdy et al.*, 1990], with observed magnetic anomalies plotted along track over the ridge flank. MAR axis is shown by north-south bold lines. Segment boundaries and labels are as in Figure 1.

data were gridded at 800 m spacing using the surface algorithm of *Smith and Wessel* [1990] with a tension factor of 0.25.

A three-dimensional inversion for crustal magnetization (Figure 3) was performed to remove skewness due to latitude and to correct for seafloor topography. We used the *Parker and Huestis* [1974] Fourier inversion method, extended to 2-D gridded data in a manner similar to Macdonald et al., [1980], which assumes a source layer of constant thickness (1 km) and an upper boundary defined by the bathymetry. Magnetization is assumed to vary laterally but to be constant with depth, and the direction of magnetization is assumed to be in the direction of the geocentric dipole (inclination=45°). The input grid of 738 x 557 points was extended out to 1024 x 1024 points using linearly interpolated borders to minimize edge effects of the Fourier transform. Band-pass filtering is required to ensure convergence toward a solution; we used a cosine-tapered band-pass filter with long- and short-wavelength cutoffs of 800 and 3.5 km and a passband of 400 to 7 km. Inversion for crustal magnetization is an inherently nonunique process. One measure of this nonuniqueness is the annihilator, which is a magnetization that produces no external magnetic field. An infinite amount of annihilator can be added or subtracted from the inversion solution without affecting the resultant magnetic field. As we will show, the true amplitudes of MAR magnetization anomalies are not properly resolved in the sea-surface data, so balancing positive to negative amplitude at reversal boundaries is not a valid method to estimate the amount of annihilator to add or subtract. Thus, to obtain the approximate location of the main anomaly zero crossings, we calculated a reduced-to-the-pole magnetic anomaly map, which involves a phase shift but no amplitude change. We then adjusted the magnetization solution by removing one times the annihilator to fit the main anomaly zero crossings of the reduced-to-the-pole map. We note, however, that this study is not sensitive to the exact amount of annihilator added or subtracted, because only relative amplitude variations in magnetization are used.

Magnetic isochrons were identified from the magnetization map using the geomagnetic polarity timescale of *Cande and Kent* [1995]. We identified both normal and reverse polarity isochrons out to chron C13n (33.25 Ma) (Figure 4). The isochron patterns are generally compatible with ridge-segmentation patterns determined from bathymetry and gravity studies [*Tucholke et al.*, 1997]. Figure 5 shows isochrons identified on representative profiles sampled from the magnetization map along flowlines calculated from stage poles of *Collette and Roest* [1992]. The profiles correlate well with a synthetic magnetic profile created at a constant spreading rate of 13 km/m.y., although they show clear variations from this rate. Interval spreading rates (Figure 6) were calculated from picks of the principal anomalies within the main spreading segments E/D, G/F, and H.

4. Geologic Setting

The ARSRP study area extends to 29 Ma crust in the northwest part of the survey and to 26 Ma crust in the southwest (Figures 1-4). It includes all or part of nine spreading segments bounded by nontransform discontinuities (NTDs), which were defined from bathymetric data, structural perturbations in sidescan-sonar records, offsets in magnetization anomalies, and gravity anomaly patterns [*Tucholke et al.*, 1997]. The NTDs are bathymetric valleys that follow irregular off-axis traces subparal-

lel to the direction of relative plate motion on the MAR flank. Bathymetric and sidescan-sonar data show marked structural perturbations of normal ridge-parallel abyssal hill fabric at the discontinuities. The discontinuities are right stepping at the MAR axis and over most of the ridge flank, although short periods of left stepping or zero offset occurred [*Tucholke et al.*, 1997, Figures 1 and 4]. At near-zero offsets, the bathymetric expression of NTDs is reduced, and at zero offsets it disappears. Offset distances ranged from 0 to 58 km (0-3 m.y.), but the only discontinuity which exceeded 30 km offset was that between segments A and E during the period ~17-11 Ma.

Sidescan-sonar, bathymetric, and gravity data show distinct IC and OC tectonic settings which extend off-axis along the old and young sides, respectively, of the NTDs [*Tucholke et al.*, 1997]. Crust at OCs and segment centers exhibits closely-spaced, linear abyssal hills and moderate- to small-throw faults. At segment centers, the linear faults and abyssal hills trend orthogonal to plate flowlines, but within 10-15 km of offsets, OC faults and abyssal hills often curve gently toward the ridge axis. RMBA gravity is moderate over OC crust and low over segment centers, suggesting normal to thickened crust, respectively, in these locations. IC tectonic settings are markedly different, exhibiting large faults with irregular orientations and large (10-20 km), quasi-circular edifices adjacent to NTDs. IC crust is also consistently elevated with respect to segment centers and OC crust, and it exhibits elevated RMBA that suggests significantly thinner crust. These IC/OC differences are consistent with studies of more global data sets of MAR ridge-axis bathymetry and RMBA gravity [*Tucholke and Lin*, 1994; *Escartin and Lin*, 1995] and with the idea that tectonic extension has asymmetrically thinned the ocean crust or exposed the mantle in IC tectonic settings [*Dick et al.*, 1981; *Karson*, 1990; *Tucholke and Lin*, 1994]. Most NTD offsets in the study area are right stepping, so the IC tectonic setting usually occurs along the southern edges of segments.

On the basis of magnetic anomaly identifications, the study area shows an overall trend of decreasing spreading rate for the past 29 m.y. (Figure 6). At 29 Ma, the MAR was spreading at a half-rate of ~17 km/m.y., which decreased slightly to ~15 km/m.y. at 27 Ma and remained constant until about 16 Ma. Rates were slightly higher from 16 to 10 Ma and subsequently have steadily decreased to a present rate of ~10 km/m.y. The slowing trend over the last 10 m.y. is consistent both with results of *Sloan and Patriat* [1992], who analyzed magnetic anomaly data just north of our study area, and with lower-resolution Kane Fracture Zone data of *Tucholke and Schouten* [1988].

A major, ~9° counterclockwise change in relative plate motion direction occurred ~24-22 Ma (Figure 4, chrons C6Cn-C6An), and it was followed by a reorganization of the plate boundary that progressed southward through the survey area. Segment F was divided into two new segments (G and H) at ~22 Ma, while to the south, segments C and D consolidated at ~20 Ma to form a single long segment (E). Farther south, segment B died out at ~19 Ma, apparently as a consequence of a steady northward migration (~2 mm/yr) of the discontinuity between segments A and B. *Sloan and Patriat* [1992] documented frequent plate motion changes of up to 11° over the last 10 m.y., and local orientation changes of similar magnitude are observed in seafloor structure and magnetic anomalies within our study area (Figure 4). Neither these changes nor those caused by local ridge propagation [*Kleinrock et al.*, 1997] have caused any significant change in segmentation pattern over the last 10 m.y.
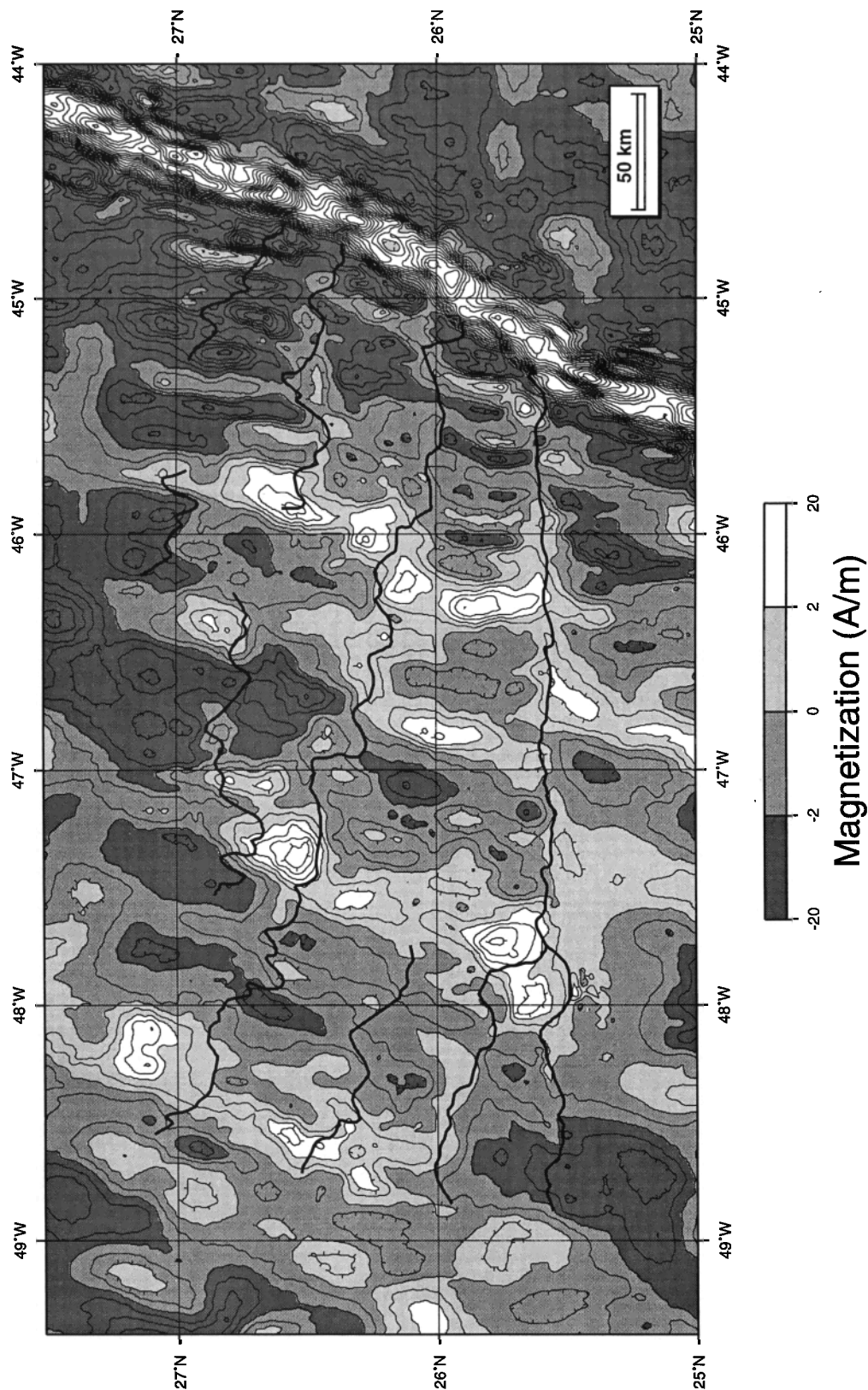
Figure 3. Crustal magnetization computed for a constant-thickness source layer of 1 km whose upper surface is defined by the bathymetry. Contour interval is 1 A/m. Main segment boundaries identified by bold lines as in Figure 1.
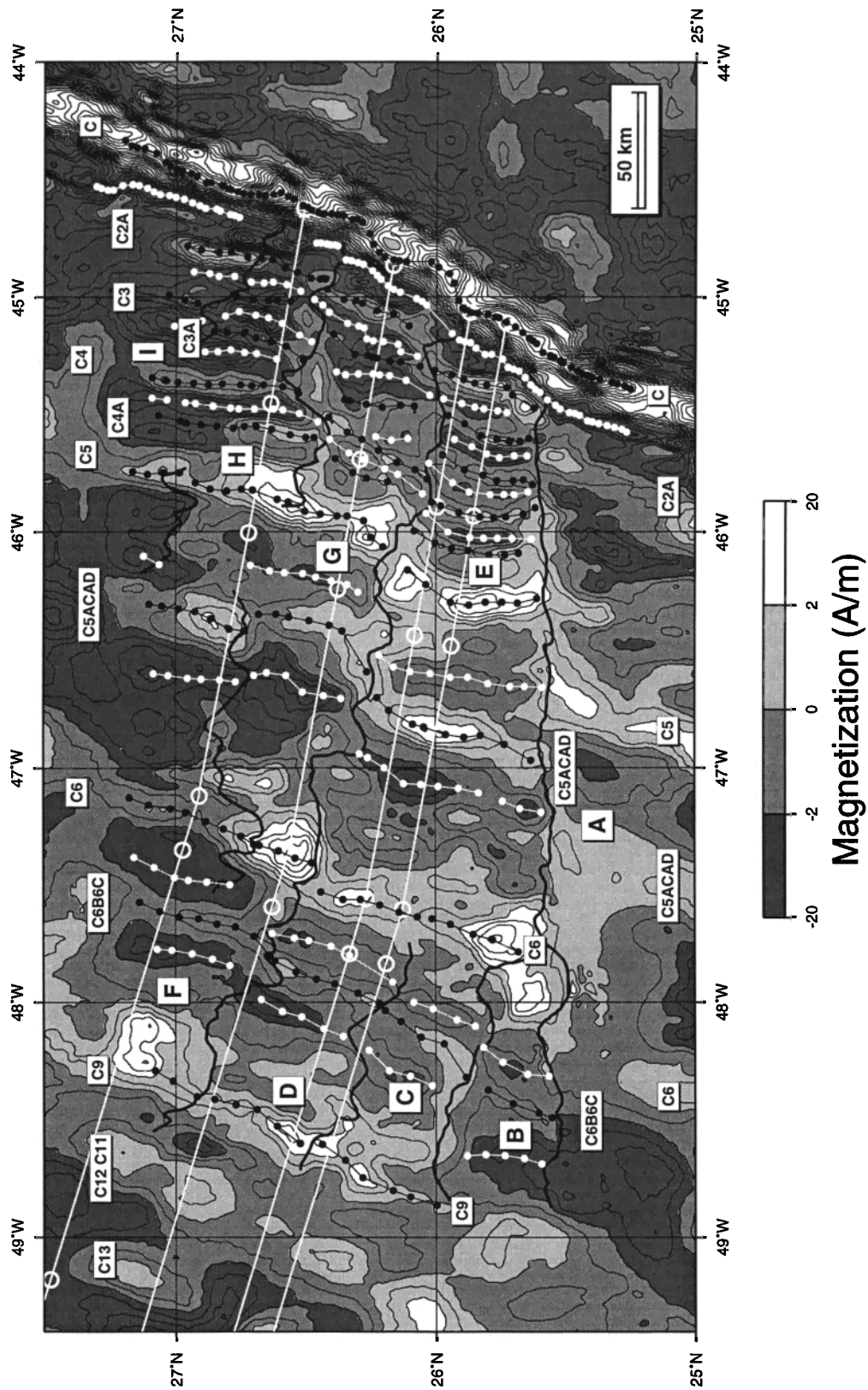
Figure 4. Magnetic isochron interpretation superimposed on the crustal magnetization map of Figure 3. Principal anomaly picks are shown by black dots (normal polarity) and white dots (reverse polarity). Main segment boundaries are shown by bold black lines. Polarity chron identifications are based on the *Cande and Kent* [1995] geomagnetic timescale. Computed flow lines based on *Collette and Roest* [1992] are shown by large white open circles and white lines.
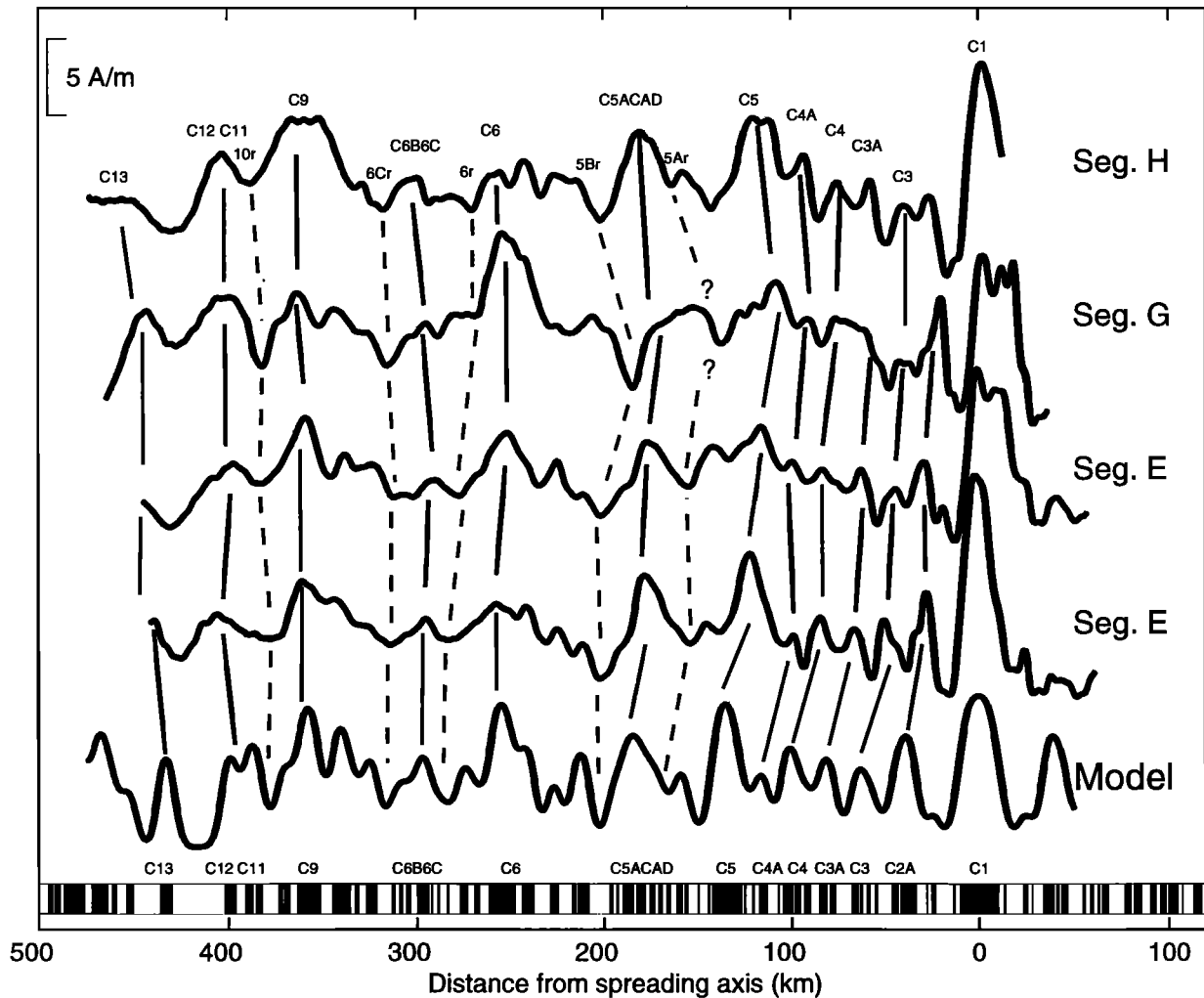
Figure 5. Four representative magnetization profiles sampled along flowlines shown in Figure 4 over the main ridge segments of the study area, compared with a forward model with constant half-spreading rate of 13 km/m.y. The model is an inversion of a synthetic magnetic field using the same inversion filters as the data. The synthetic magnetic field was computed assuming flat bathymetry at -3.5 km depth and a square-wave magnetization that was Gaussian filtered (sigma 4 km) to simulate the effects of crustal accretion.

5. Magnetic Results

5.1. Magnetization Decay With Age

Investigation of magnetization amplitude as a function of crustal age in our study area is complicated by the fact that the amplitude of crustal magnetization anomalies changes substantially along isochrons. For the purpose of discussion, we chose to examine the mean amplitude of the magnetization averaged along major isochrons within each ridge segment. Other approaches, such as using magnetization values along segment centers, are equally valid but show the same basic results. Isochron-averaged magnetization plotted against age (for normal polarities only) is shown for segment E/D in Figure 7. The other ridge segments in the study area show similar patterns of amplitude change with age. We use magnetization rather than magnetic field because this removes any phase shift due to latitude, and it takes into account the effect of deepening seafloor with age. Our data show patterns consistent with previous observations in the Atlantic. For example, over 0-5 Ma crust, there is a marked decrease in magnetic anomaly amplitude like that observed in the South Atlantic [*Wittpenn et al.*, 1989], in the Mid-

Atlantic Ridge at Kane (MARK) area south of Kane Fracture Zone [*Pockalny et al.*, 1995], and in a survey around Atlantis Fracture Zone [*Pariso et al.*, 1996]. Anomaly C5n also has a strong magnetization like that observed in other MAR surveys [e.g., *Pockalny et al.*, 1995; *Pariso et al.*, 1996].

Initial inspection suggests that a magnetization-decay time of 1.5 m.y., as suggested by *Pockalny et al.* [1995], might be a good fit to the data (Figure 7a, bold-dash-dot line). However, anomalies C5n, C6n, and C9n show relatively high magnetization that is clearly inconsistent with this decay curve. We suggest that anomalies C5n, C6n, and C9n are actually the most accurate representation of off-axis crustal magnetization, and that low magnetization estimates for other crust (notably anomalies C2An-C4n) are artifacts caused by the lack of resolution in sea-surface data due to the filtering effect of water depth and reversal spacing. To illustrate this point, we constructed a forward model to show the resolution limitations of the data (Figures 7c and 7d). The forward model assumes a constant spreading rate of 13 km/m.y. and an input geomagnetic timescale [*Cande and Kent*, 1995] in the form of a square-wave magnetization function that is passed through a Gaussian filter (4-sigma = 16 km) to simulate
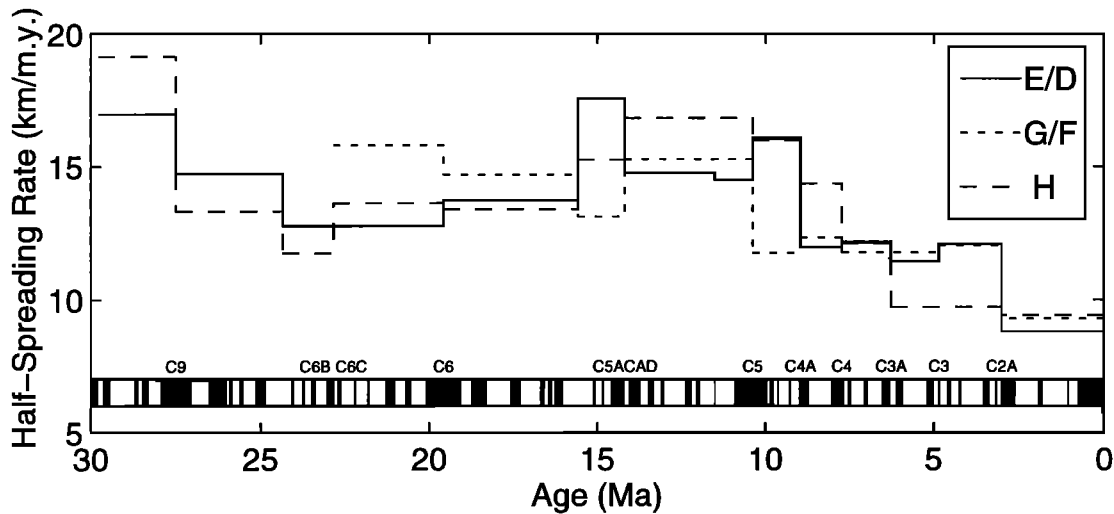
Figure 6. Plot of interval half-spreading rates for the three main ridge segments of the study area.

effects of the crustal accretion process [*Schouten and Denham*, 1979]. The resultant magnetization function was used to compute the magnetic anomaly at the sea surface for a flat source layer (3.5 km depth and 1 km thick) and then inverted for magnetization using the same filter parameters as for the measured data. The model magnetization (Figure 7d) successfully reproduces the resolution of individual anomalies found in the observed data (Figure 7b) for crust younger than ~15 Ma (see also Figure 5). A loss in anomaly resolution with age is apparent in observed data over older crust (Figure 7b); this may be an effect of long-term magnetization decay. Significantly, the model does not incorporate any decay in magnetization with age; yet if we pick peak amplitudes of the major anomalies (Figure 7c), we readily observe rapid apparent decay in anomaly amplitude from
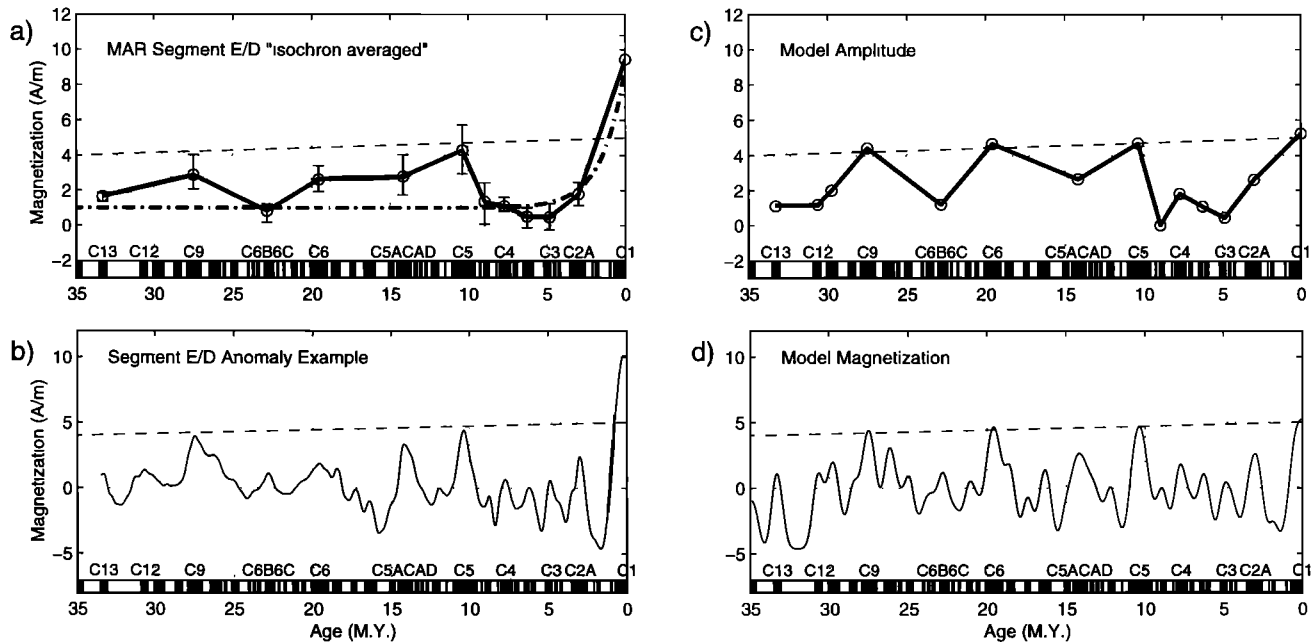

Figure 7. (a) Observed crustal magnetization amplitude versus age for segment E/D. Magnetization has been averaged along normal polarity isochrons within the segment, and error bars indicate the total range in along-isochron value. Bold-dashed line shows magnetization-decay model of *Pockalny et al.* [1995], which assumes a 1.5 m.y. decay time. Light-dashed line shows "long-term decay," which is based on anomalies C1n, C5n, C6n, and C9n in model Figure 7d and which is actually an artifact (see text). (b) Representative profile from segment E/D with identification of the principal normal polarity isochrons. Light-dashed line as in Figure 7a. (c) Normal polarity isochron amplitude picked from a constant-magnetization forward model shown in Figure 7d. Note the severe loss of amplitude over the chron C2n-C4An interval; this is a function of poor sea-surface resolution of short, closely spaced reversals. Light-dashed line as in Figure 7a. (d) Forward model of crustal magnetization. A sea-surface magnetic field anomaly was computed on the basis of a constant-amplitude square-wave input magnetization of 5 A/m for a half-spreading rate of 13 km/m.y., filtered using a Gaussian filter (sigma 4 km) and inverted for crustal magnetization using the same filters as used on the measured data.
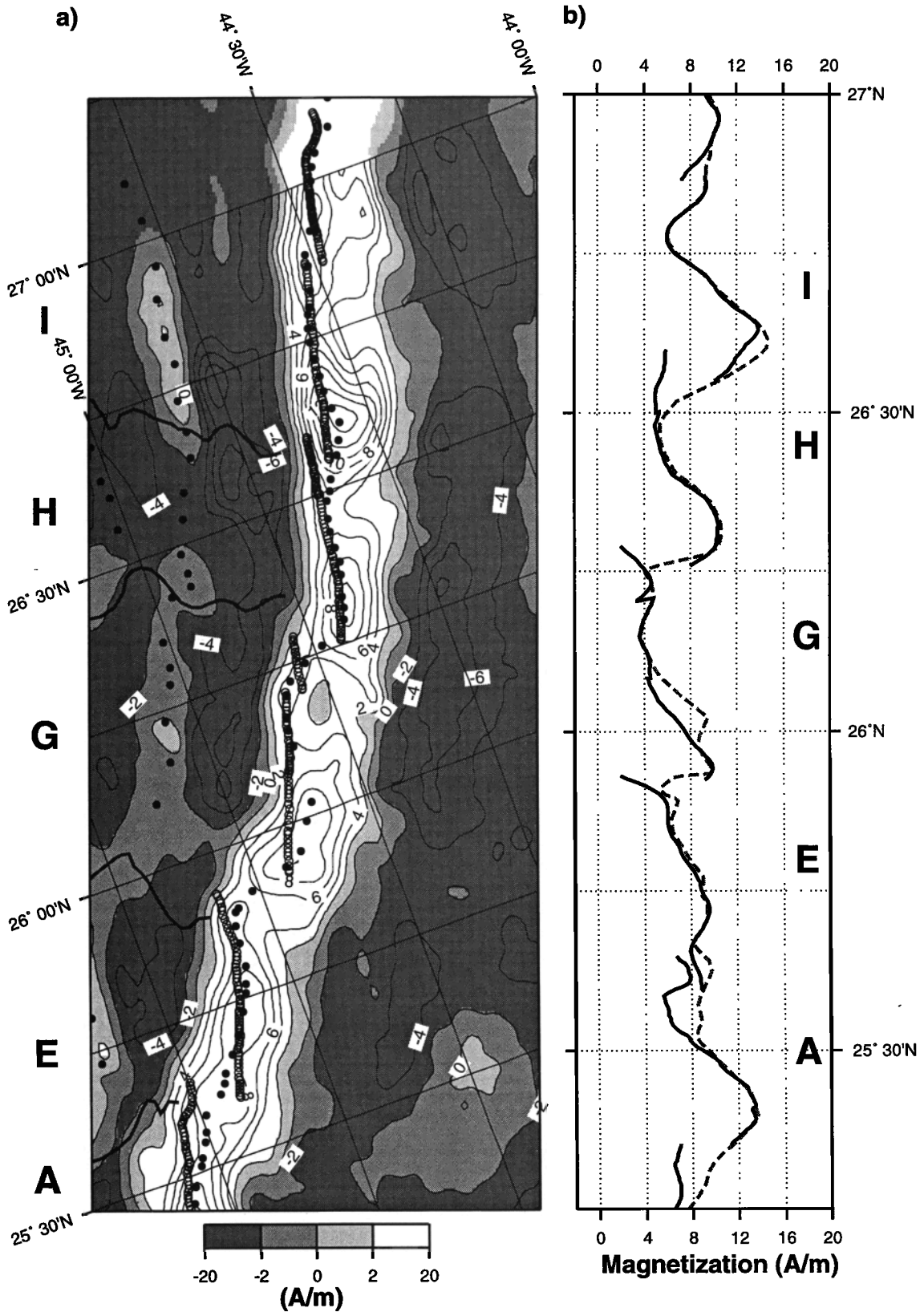
Figure 8. (a) Contour map of magnetization in the axial region of the MAR (2 A/m contours), with the neovolcanic axis (open circles) picked from morphology [*Smith and Cann*, 1992] and the trend of the maximum magnetization anomaly shown by filled circles. Spreading segments identified by letters as in Figure 1. (b) Magnetization picked along the axis of the maximum magnetization anomaly (dashed line) and along the neovolcanic axis (solid lines). Note the distinct segment-scale asymmetry from north to south, with greater magnetization at the southern ends of spreading segments.

the axis to anomaly C4An and apparent decay at older periods around anomalies C5ACn-C5ADn and C6Bn-C6Cn. This pattern is very similar to the observed data (Figure 7a). The high amplitudes of anomalies C5n, C6n, and C9n are thus the most accurate estimates of crustal magnetization intensity, and a decay rate extracted from the apparent magnetization decrease from anomaly C1n into the anomaly C2n-C4An reversal sequence is meaningless. That is not to say that there is not a real and very large near-axis decay in magnetization. The reality of such short-term decay is well documented [e.g., *Macdonald*, 1977; *Johnson and Atwater*, 1977; *Gee and Kent*, 1994; *Johnson and Tivey*, 1995; *Hussenoeder et al.*, 1996], even though there is significant uncertainty about the magnitude and rate of the effect.

We also note that even relatively long intervals of constant polarity (chrons C5n, C6n, and C9n) suffer from the filtering effect (Figures 7a and 7c, light-dashed line). The apparent long-term trend of decreasing magnetization present in the forward model suggests a decrease of 1 A/m over a 35 m.y. period for an initial 5 A/m magnetization (i.e., a 20% loss in original amplitude). We cannot resolve real long-term decay that occurs at a rate less than indicated by this artifact. Observed data (Figure 7a) suggest a long-term decay of up to 3 A/m over a 35 M.y. period; however, this decay is within the uncertainty of the amplitude estimates and is not distinguishable from the long-term decay artifact.

5.2. Axial Crustal Magnetization

Along-axis variability in crustal magnetization at the present spreading axis was examined in two axial profiles (Figure 8), one following the neovolcanic axis as defined by seafloor morphology [*Smith and Cann*, 1992] and the other following the magnetic axis, defined as the maximum magnetic anomaly amplitude of the central anomaly magnetic high (CAMH). The magnetic axis is poorly resolved in sea-surface data, but it appears to follow the morphologic axis quite closely. The coincidence of these features is consistent with studies of near-bottom magnetic profiles on the MAR [e.g., *Macdonald*, 1977; *Hussenoeder et al.*, 1996] which find that the CAMH is closely associated with the neovolcanic axis, which most likely represents the time-averaged axis of crustal accretion. A distinct along-axis asymmetry in magnetization is observed in both profiles, with the southern ends of ridge segments being more magnetic than the northern ends (Figure 8b). The same asymmetry is observed at the MAR axis between 28°N and Atlantis Fracture Zone, but it does not appear north of the fracture zone [*Pariso et al.*, 1996] nor is it present near the Kane Fracture Zone [*Pockalny et al.*, 1995; *Hussenoeder et al.*, 1996; M. A. Tivey and H. Schouten, unpublished data, 1990].

5.3. Off-Axis Crustal Magnetization

To investigate how along-isochron variation in magnetization changes with age, we studied off-axis, along-isochron variations in crustal magnetization amplitude for both normal and reverse polarity isochrons. Figures 9 and 10 show these variations plotted relative to the mean along-isochron magnetization. Normal polarity isochrons (Figure 9) exhibit considerable variability in magnetization both along isochrons and between segments. Furthermore, the marked south-to-north asymmetry found in the axial magnetization (Figure 8) does not continue consistently off-axis, except perhaps in segments H and I. Reverse polarity isochrons (Figure 10) show a more systematic pattern, consisting of strong reversed magnetization at segment centers and weaker

reversed magnetization toward segment ends. Thus reverse polarity crust is apparently less magnetic at segment ends (i.e., near discontinuities) than at segment centers. This pattern is opposite to what is typically observed at ridge axes (normal polarity), which have stronger magnetization toward segment ends [e.g., *Grindlay et al.*, 1992; *Pariso et al.*, 1996; *Weiland et al.*, 1996]. As expected from magnetization decay with age, both normal and reverse polarity amplitude variations are reduced compared to amplitude variations along-axis (Figures 8-10).

To better understand the spatially averaged patterns of crustal magnetization, we normalized along-isochron magnetization amplitude by dividing by the maximum range of the along-isochron amplitude for each isochron shown in Figures 9 and 10. We offset the resultant values so that the minimum along-isochron value is zero and the maximum magnetization (in a positive polarity sense) is one. The normalized curves were parameterized into unit segment length and stacked according to their polarity, i.e., normal or reverse polarity (Figures 11b and 11c). For comparison, we similarly stacked the along-axis variations to highlight the asymmetrical pattern of higher magnetization toward the southern ends of segments (Figure 11a). Off-axis, normal polarity crust (Figure 11b) has a weak trend of slightly higher magnetization toward the south, but this is only marginally significant at the one standard deviation level. In marked contrast, reverse polarity crust (Figure 11c) shows strong and significant (beyond one standard deviation) along-isochron variation, with highly magnetized crust (in a reverse polarity sense) at segment centers compared to segment ends. This off-axis, reverse polarity magnetization pattern is remarkably different from that of normal polarity magnetization either on-axis or off-axis.

The contrasting behavior between normal and reverse polarity crust at first appears to be a paradox. If, however, we view the along-isochron magnetic trends in terms of their "positiveness," then the paradox is resolved. Near segment ends, normal polarity crust is more positive and thus more magnetic in the present field, but reverse polarity crust is more positive and thus less magnetic (Figure 11). The extra positive magnetization represents only a small percentage increase in total magnetization for normal polarity crust, but for reverse polarity crust, the extra positive magnetization is opposite to the original magnetization and represents a significant decrease in total magnetization. This positiveness is characteristic of an induced component of magnetization, and it would appear that much of the original remanent magnetization is destroyed toward segment ends and replaced with induced magnetization. Similar observations of relatively positive magnetization near segment ends have also been made over the MAR south of Kane Fracture Zone [*Pockalny et al.*, 1995] and between 28°N and the Atlantis Fracture Zone [*Pariso et al.*, 1996].

To assure that these along-isochron trends in magnetization are robust, we must address the limitations of the data, which include edge effects as well as filtering effects of both the analysis methods and the gridding process. Magnetic anomalies arise from contrasts in magnetized material, so that the maximum anomalies will decrease away from the edges of magnetized blocks. This behavior is well demonstrated by the propensity of sea-surface magnetic anomalies to have a "hat-shaped" character in conventional cross-isochron profiles [*Vine*, 1966]. Similarly, along isochrons, the juxtaposition of blocks of different polarities across an NTD can create strong edge effects that result in anomaly asymmetry within polarity blocks of a spreading segment [e.g., *Collette et al.*, 1974; *Kent et al.*, 1978]. Both reverse and normal polarity blocks show strong magnetic anomalies at·
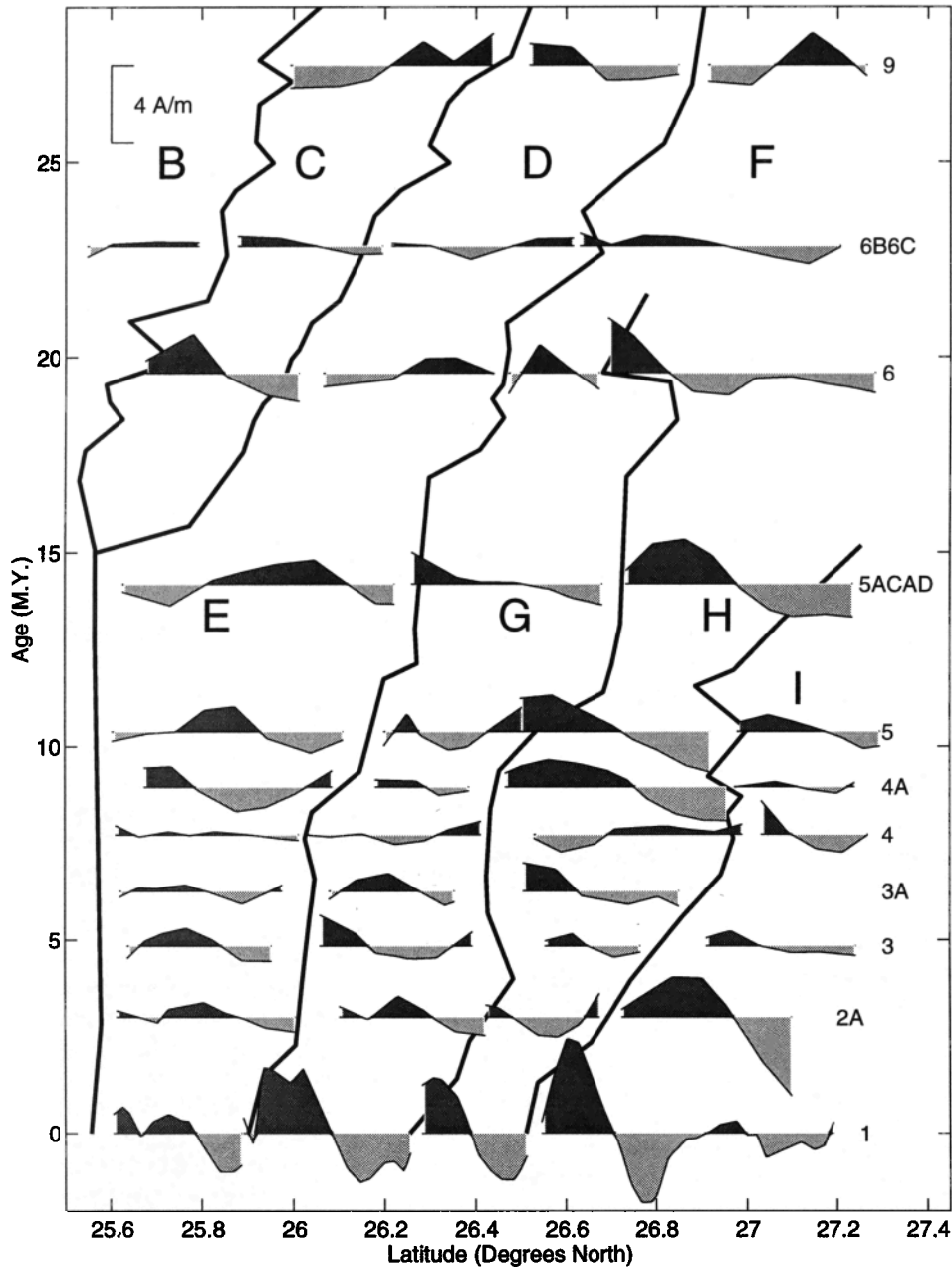
Figure 9. Plan view of normal polarity, along-isochron variation in crustal magnetization for isochrons (labeled), relative to the mean isochron value. Dark gray is more magnetized than the isochron mean, and light gray is less magnetized than the isochron mean. Bold lines show discontinuities between segments, which are lettered as in Figure 1. Note that there is no overall along-isochron trend within segments.

their boundaries, and the anomalies decrease in amplitude or "sag" into the interior of the block. The wavelength of this sag is proportional to the length of the block or spreading segment. Thus, to successfully invert for magnetization, it is imperative that the filtering does not adversely affect the wavelength of any segment-length variations in magnetic field or magnetization. Our long-wavelength cutoff was tapered between 800 and 400 km, allowing us to resolve along-isochron trends in magnetization without introducing artifacts due to filtering. The longest ridge segment within the survey area is ~100 km long. Our short-wavelength cutoff, tapered from 7 to 3.5 km, also limits the effect of filter sidelobes and edge effects. Thus, within the usual constraints of the inherently nonunique inversion approach, the ob-

served segment-scale, along-isochron variations in crustal magnetization appear to be valid.

5.4. Magnetization in Relation to Tectonic Setting

Previous studies have discussed hypotheses for the above kinds of segment-scale variations in crustal magnetization, but asymmetries related to IC/OC tectonic setting have not been specifically investigated. In our study area, ridge-flank segmentation is relatively well defined by bathymetric, gravity, and magnetic data, allowing us to address this question. The detachment-fault hypothesis suggests that as oceanic crust forms at a slow-spreading ridge axis, upper crust is preferentially transported to the outside corners, and lower crust and upper mantle are ex-
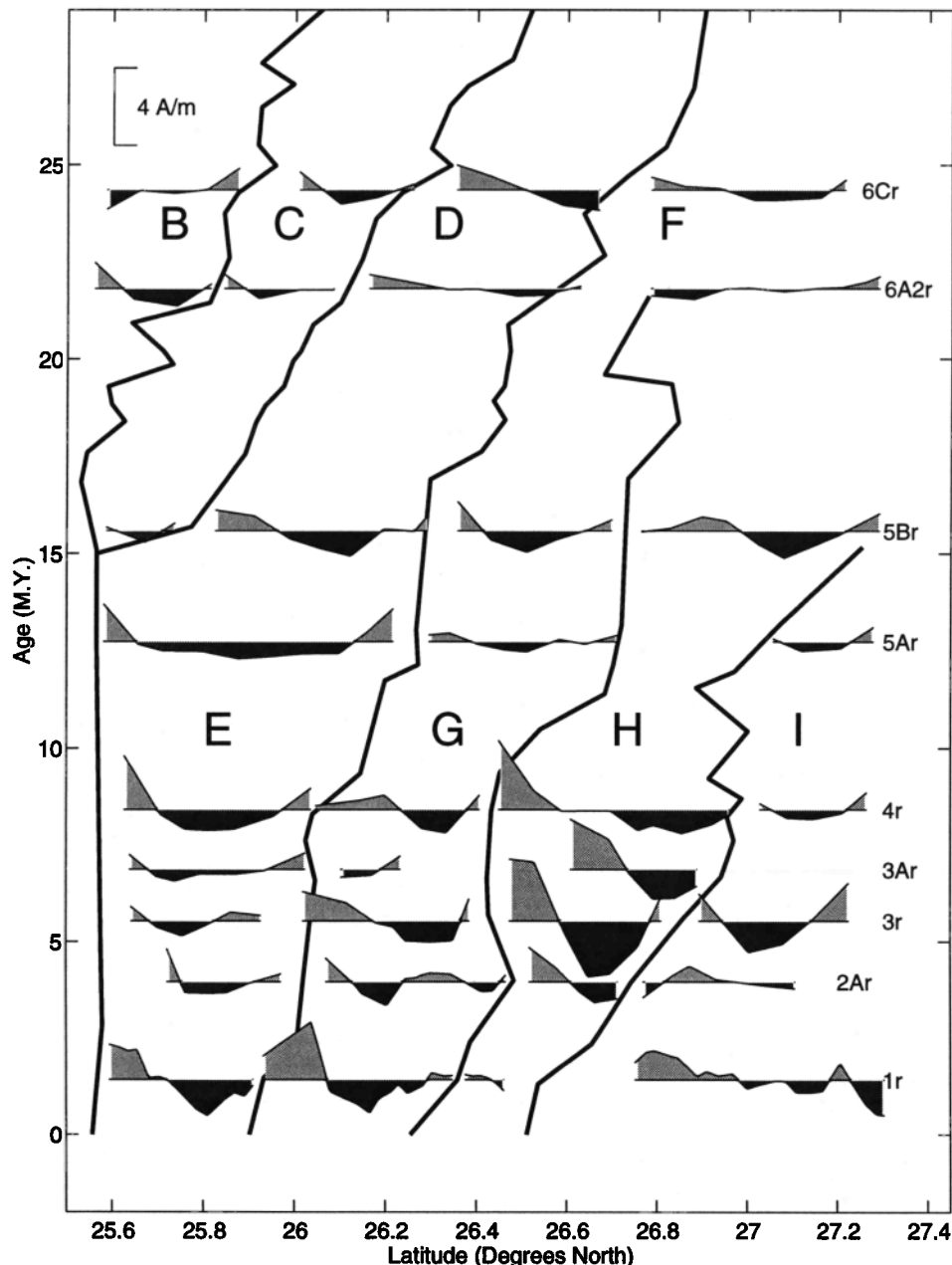
Figure 10. Plan view of reverse polarity, along-isochron variation in crustal magnetization for isochrons (labeled) relative to the isochron mean. Dark gray is more magnetized (i.e., more reversely magnetized) than the isochron mean, and light gray is less magnetized (i.e., more positive) than the isochron mean. Bold lines show discontinuities between segments, which are lettered as in Figure 1. Note the systematic tendency toward more positive magnetization near discontinuities.

posed at inside corners [*Dick et al.*, 1981; *Karson*, 1990; *Tucholke and Lin*, 1994]. The extrusive layer of the upper crust is known to be highly magnetic, and it undoubtedly contributes a significant part of the magnetic signal in young crust [*Talwani et al.*, 1971; *Harrison*, 1987; *Tivey*, 1996]. If the extrusives tend to be removed from inside corners, thus exposing what are thought to be less magnetic gabbros and peridotites, then one should expect to see an IC/OC asymmetry in crustal magnetization, with OC crust being significantly more magnetic than IC crust.

We tested this hypothesis by analyzing magnetization with respect to IC/OC tectonic setting within segments. We divided each along-isochron profile (Figures 9 and 10) into one-thirds

(northern, central, and southern) and classified each isochronal portion according to its tectonic setting (i.e., IC, segment center, or OC). These magnetization values were then plotted versus age (Figure 12). While there is a large variation with age as discussed earlier (see Figure 7), for normal polarity chrons, there is no consistent difference in magnetization of IC and OC crust nor in magnetization of these areas compared to segment centers. For reverse polarity crust, there is a trend toward more positive magnetization of both IC and OC crust compared to segment centers, as expected from our previous discussion (Figure 11).

We further examined potential correlations between IC/OC tectonic setting and crustal magnetization in a less direct way, by
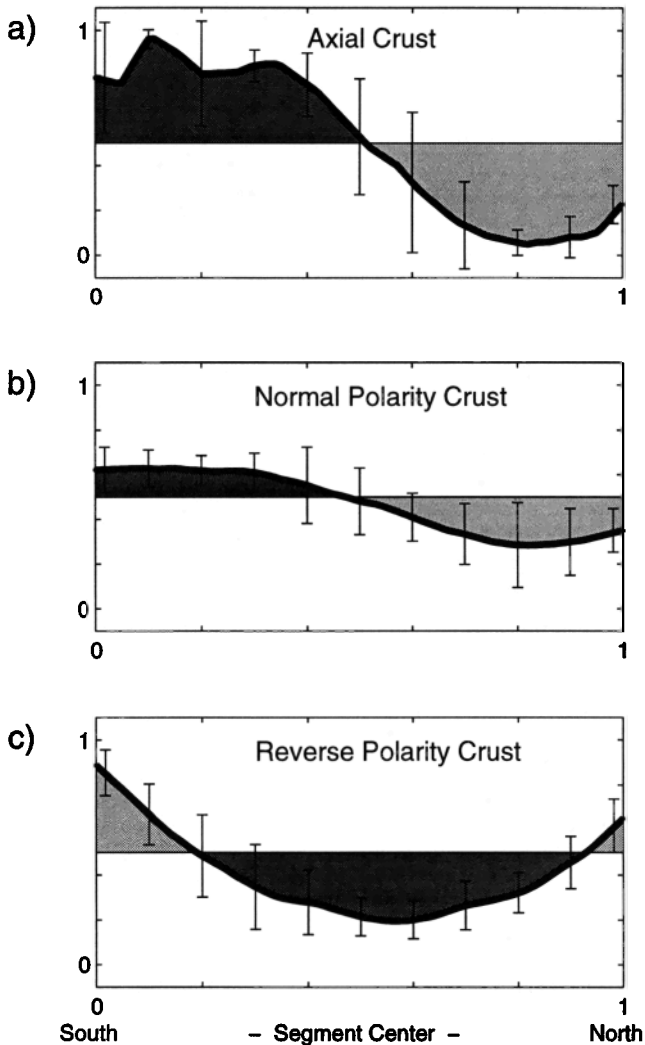
Figure 11. Stacked, along-isochron variation in crustal magneti-zation, averaged as described in text. The vertical axis is the nor-malized along-isochron magnetization, with 1 representing the maximum magnetization value in a positive polarity sense and 0 representing the minimum value. The horizontal axis is normal-ized to unit segment length. Error bars are one standard devia-tion from the mean for every tenth value. Dark gray shading shows more magnetized crust and light gray shading shows less magnetized crust as explained in Figures 9 and 10. (a) On-axis variation in crustal magnetization, showing stronger magnetiza-tion toward the south. (b) Off-axis normal polarity isochronal variation, which shows weak along-axis variation at one standard deviation. (c) Reverse polarity isochronal variation which shows a significant trend to more magnetized crust at segment centers.

comparing RMBA gravity and magnetization. Elevated RMBA gravity is thought to indicate thin crust and correlates strongly with IC tectonic settings in the study area, while moderate and low RMBA gravity values typify more normal crust associated with OC and segment-center tectonic settings, respectively [*Tucholke and Lin*, 1994; *Escartin and Lin*, 1995]. The RMBA map of *Tucholke et al.* [1997] was sampled along isochrons (Figure 4), and colocated values of gravity and magnetization were plotted against one another in three plots: on-axis, off-axis normal polarity, and off-axis reverse polarity (Figure 13). We did not normalize for the effects of magnetization decay or amplitude

resolution, which contributes to scatter in the plotted data. On-axis, there is a weak negative correlation of decreasing magneti-zation with increasing RMBA (Figure 13a), suggesting that thin-ner crust correlates with reduced magnetization, although this correlation (correlation coefficient, r = 0.17, for number of sam-ples, N = 53) is not statistically significant at the 95% confidence level. Off-axis (Figure 13b), magnetization of normal polarity isochrons shows a weak positive correlation with RMBA, i.e., thinner crust has slightly higher (more positive) magnetization. This correlation (r = 0.405 for N = 283) far exceeds the 1% chance that it is a random occurrence, and it thus is highly statis-tically significant at the 99% confidence level. The residual gravity anomaly thus predicts ~16% (i.e., 0.405^2) of the variation in magnetization, with other factors, such as noise, contributing the remaining 84%. Off-axis magnetization for reverse polarity crust (Figure 13c) shows that increasing RMBA correlates with less reversely magnetized crust; that is, thinner crust again corre-lates with more positively magnetized crust. The correlation coefficient (r = 0.18 for N = 266) exceeds the 95% confidence level, so the trend is statistically significant. Thus we can con-clude that there is no statistically significant correlation between axial magnetization and RMBA (or apparent crustal thickness), but there is a significant correlation off-axis, with thinner crust of both polarities being more positively magnetized. This off-axis trend confirms our prior analyses that progressively thinner crust (i.e., from segment center to OC or IC) has increasingly positive magnetization. However, this is opposite to what we expect if off-axis magnetism resides primarily in extrusive crust. The implications of this finding are discussed below.

6. Discussion

6.1. Isochronal Trends in Crustal Magnetization

Our results show that in off-axis crust, along-isochron mag-netization exhibits a distinct and systematic shift to more positive magnetization near segment ends for reverse polarity crust and very weak variations in normal polarity crust (Figure 11). The shift to more positively magnetized crust near segment ends re-gardless of polarity, as opposed to simply more magnetized crust, is consistent with previous studies [*Pockalny et al.*, 1995; *Pariso et al.*, 1996]. It rules out FeTi or other geochemical variations as possible reasons for this variation, and it strongly suggests the presence of an induced component of magnetization. In Figure 14, we show the effect of adding a component of induced mag-netization preferentially to segment ends, assuming that remanent magnetization has no along-isochron variation and has equal but opposite magnitude for normal and reverse polarity crust, respec-tively. The result is that normal polarity crust would show in-creased positive magnetization at segment ends, while reverse polarity crust would show decreased reversed magnetization (Figure 14c). This model can be used to separate induced and remanent magnetization components by considering the sum and the difference of the normal and reverse polarity variations as illustrated in Figure 14d. By adding the normal (N) and reversed (R) variations and dividing by two (Figure 14d, left), we obtain the induced component. The difference between the normal and reversed variations divided by two (Figure 14d, right) provides the remanent component.

We applied this procedure to the normal and reverse polarity trends that were calculated in Figures 11b and 11c, and the re-sults are shown in Figure 15. We find that induced magnetiza-tion increases toward segment ends as previously suggested
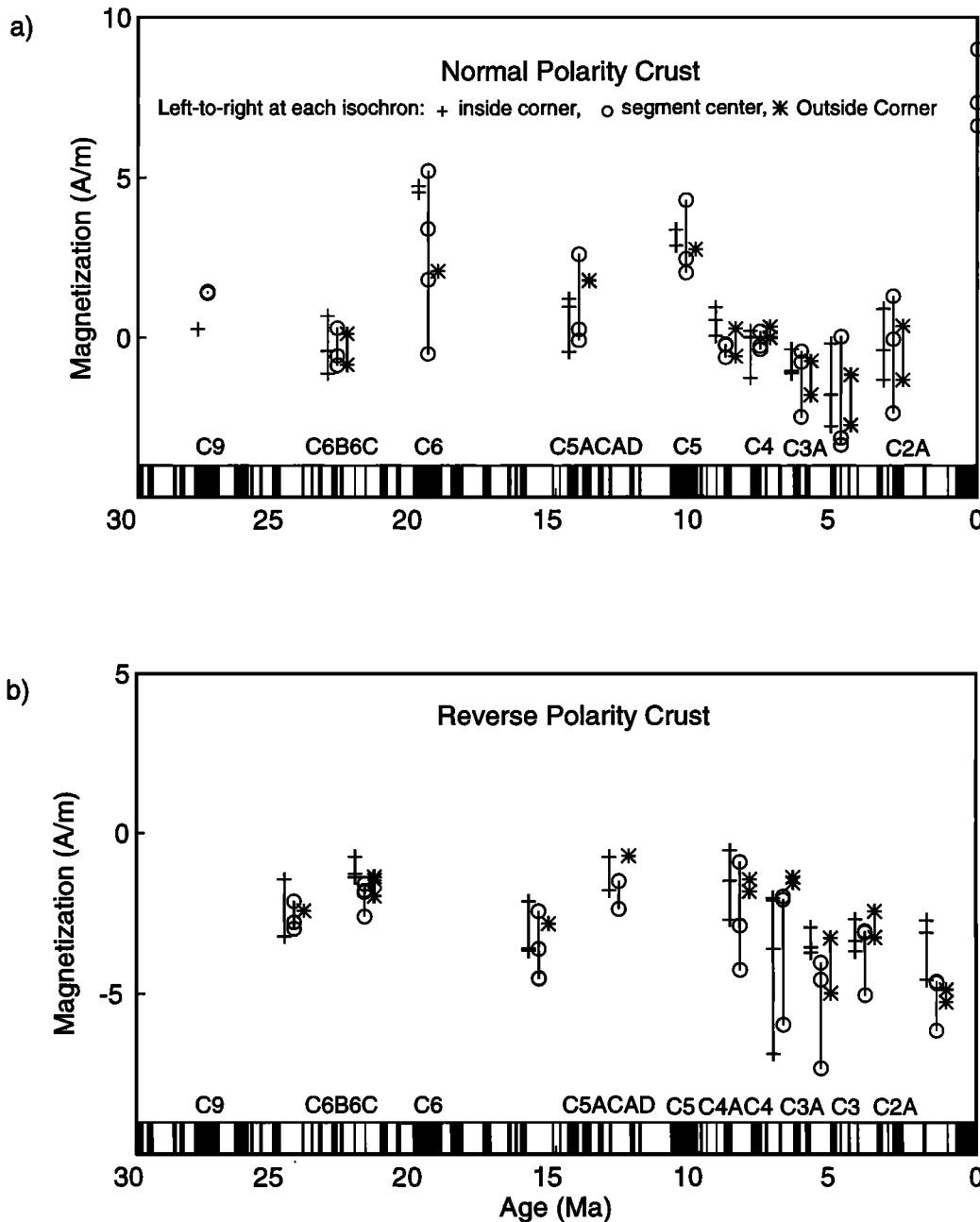
a)

Normal Polarity Crust

Left-to-right at each isochron: + inside corner, o segment center, ✳ Outside Corner

Magnetization (A/m)

10

5

0

C9   C6B6C   C6   C5ACAD   C5   C4 C3A   C2A

30   25   20   15   10   5   0

b)

Reverse Polarity Crust

Magnetization (A/m)

5

0

-5

C9   C6B6C   C6   C5ACAD C5C4AC4 C3A C3 C2A

30   25   20   15   10   5   0

Age (Ma)

Figure 12. Crustal magnetization estimates for inside corner (IC), segment center, and outside corner (OC) crust at discrete isochrons, plotted against crustal age. Each symbol is a mean value for one isochron in one segment, and vertical lines show the range of values. (a) Magnetization estimates for normal polarity isochrons. (b) Magnetization estimates for reverse polarity isochrons. As expected, there is a tendency for segment ends (IC and OC crust) to be slightly more positively magnetized than segment centers.

(Figure 15a). There is also a slight asymmetry in the curve, with greater induced magnetization toward the southern ends of segments, which are predominantly IC crust in our study area. As noted earlier, IC crust tends to be thin, and in our analysis of RMBA versus magnetization in Figure 13, it is suggested that thin IC crust should be more positively magnetized than thick crust.

Both *Pockalny et al.* [1995] and *Pariso et al.* [1996] invoked induced magnetization as the source of the positive magnetization near segment ends, but they disagreed on where this magnetization might reside. *Pockalny et al.* [1995] considered that induced magnetization in serpentinized lower crust (i.e., gabbro) gives

rise to enhanced magnetization in the normal polarity direction. On the basis of the results of *Dunlop and Prevot* [1982] and *Pariso and Johnson* [1993a], however, *Pariso et al.* [1996] suggested that altered gabbros have a stable magnetization that is remanent rather than induced, and they proposed that serpentinized mantle must provide the additional induced magnetization. Further studies are needed to fully characterize the magnetization of oceanic gabbros and to determine the degree to which they may be a source of remanent and or induced magnetization.

We have discussed the enhanced positive magnetization as being induced magnetization, but it is equally possible that it is viscous remanent magnetization, a time-dependent magnetization
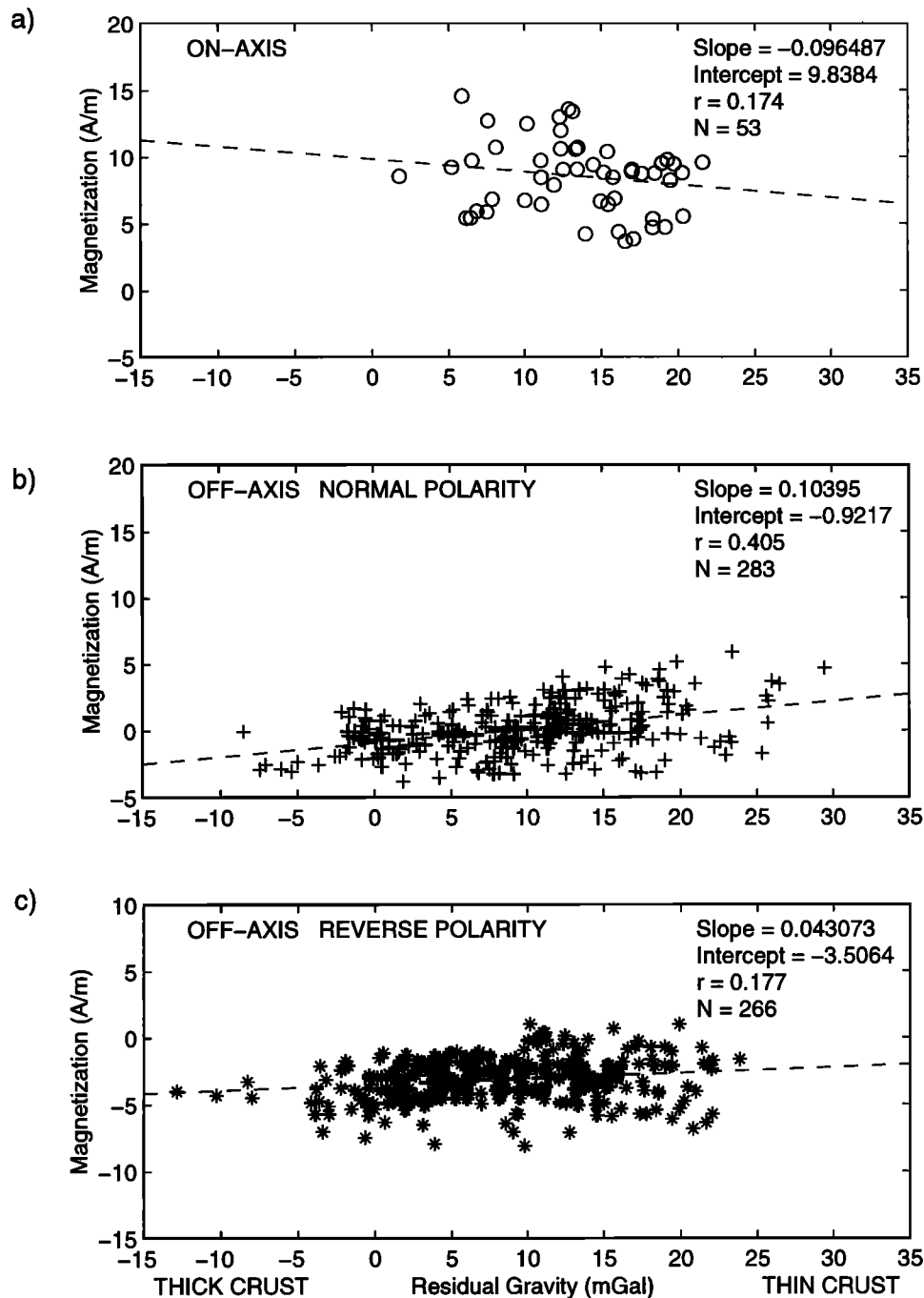
Figure 13. Plots of crustal magnetization versus residual mantle Bouguer gravity anomaly in the study area, derived as discussed in text. (a) On-axis normal polarity crust. (b) Off-axis normal polarity crust. (c) Off-axis reverse polarity crust.

that grows logarithmically with time in the direction of the Earth's field. Viscous remanence is common in magnetite-bearing rocks [*Dunlop*, 1973], and it therefore could be important in serpentinites, especially those with fine-grained magnetite [*Tivey and Johnson*, 1984]. Models of lithosphere formation also show that viscous magnetization could contribute significantly to the source of magnetic anomalies and in part could be responsible for their skewness [*Arkani-Hamed*, 1988, 1989]. Without samples, it is not possible to determine whether the positive magnetization at segment ends is induced or viscous, but the effect on the magnetic field is the same in either case.

The computed remanent component of magnetization is shown in Figure 15b. There is a weak but systematic along-isochron variation in remanence, with less remanent magnetization toward segment ends. Unlike induced magnetization, there is no clear asymmetry in remanent magnetization that can be attributed to IC/OC crustal variations. Furthermore, the pattern of along-isochron remanent magnetization (Figure 15b) is distinctly different from the pattern of presumably remanent magnetization on-axis (Figure 11a), suggesting that the source responsible for the axial magnetization pattern is severely attenuated off-axis.
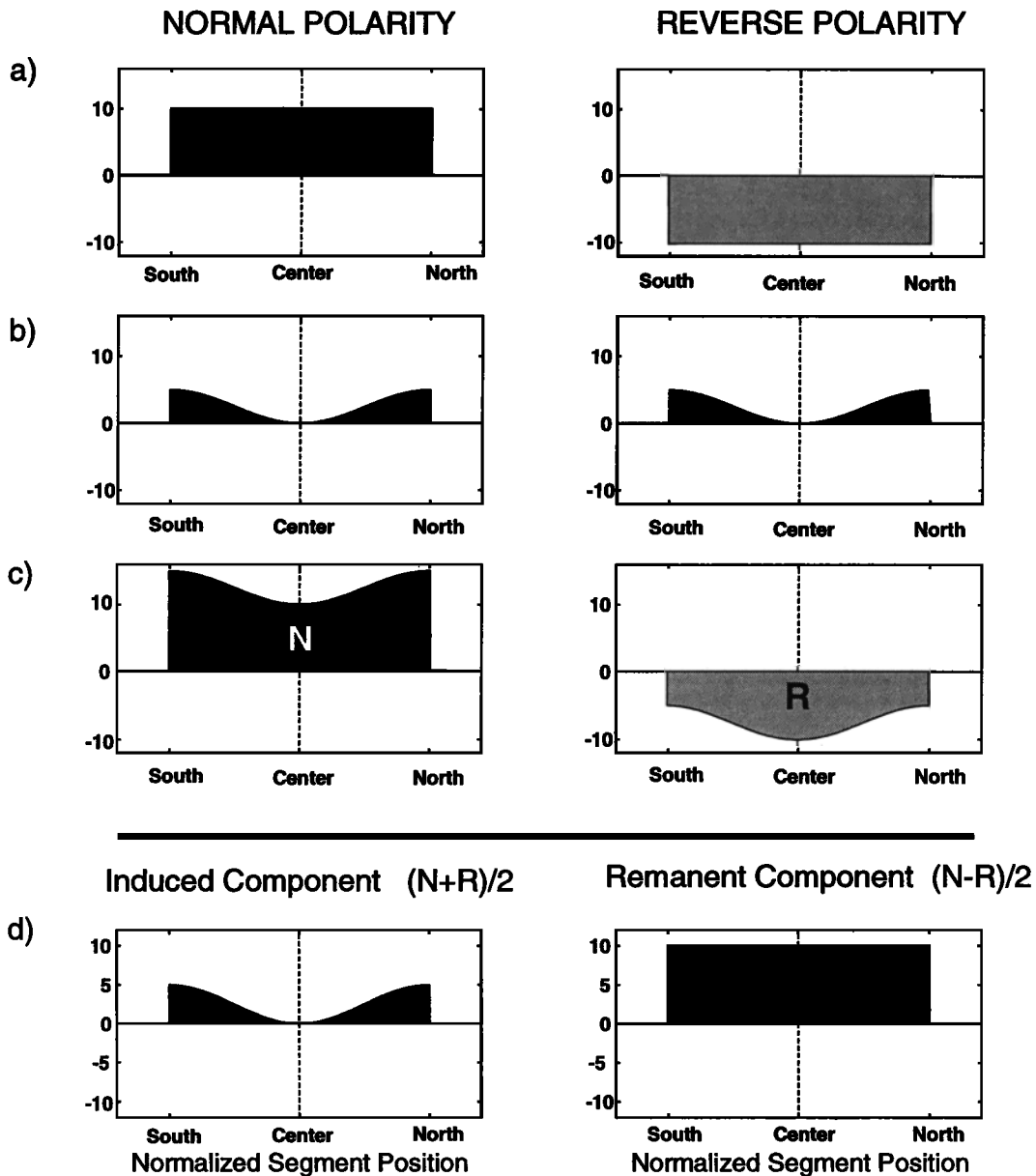
Figure 14. Schematic model showing the effects of adding an induced remanence to segment ends in both normal and reversely magnetized crust. (a) Normal and reversely magnetized crustal remanence of equal but opposite polarity. (b) Induced component that is always in the direction of the present-day field, i.e., positive. (c) Sum of induced and remanent components showing the enhanced positive magnetization in normal polarity crust and reduced reverse magnetization in reversely magnetized crust. (d) Arithmetic sum (left) and difference (right) of the normal and reverse polarity signals, divided by two, showing how the magnitude of the induced component (left) and the magnitude of the remanent component (right) are recovered.

6.2. Implications for the Source of Crustal Magnetization

On-axis to off-axis changes in remanent magnetization patterns allow us to investigate the sources of crustal magnetization. If we assume that extrusive lavas provide the primary source of off-axis magnetization, then magnetic remanence patterns (Figure 15b) show that the off-axis extrusive layer at segment ends is either thinned and/or its magnetization is preferentially destroyed. RMBA gravity and dredged serpentinite in our study area suggests strong crustal thinning and removal of extrusives along inside corners [*Tucholke et al.*, 1997]. At outside corners, the gravity data suggest significantly thicker crust than at inside corners, but we do not know the thickness of the extrusive section.

Extrusive thickness may vary roughly in proportion to total crustal thickness, it may have relatively constant thickness despite thickness variations in the underlying layer 3 crust [e.g., *Tolstoy et al.*, 1993], or it may thin because of limited melt input near the NTD [*Cannat*, 1993]. Only the last case would cause reduced OC crustal remanence; even then, the layer would need to have near-zero thickness to explain the remanence symmetry with IC ends of segments. While there may well be OC thinning of the extrusive layer, it is unlikely to approach zero thickness.

Preferential destruction of remanent magnetization in the extrusive layer at segment ends is also possible, but there is no obvious reason why this should occur. Wherever present within a
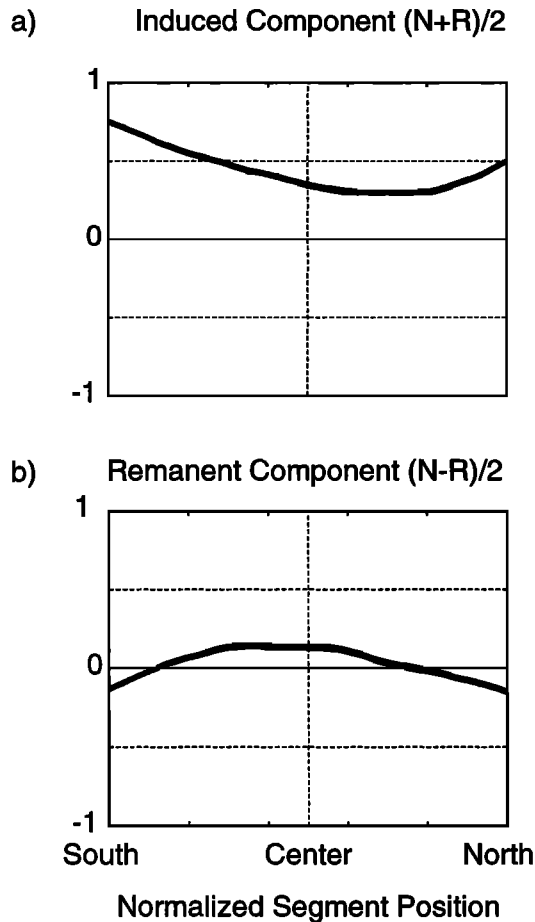
a)   Induced Component (N+R)/2

b)   Remanent Component (N-R)/2

South   Center   North

Normalized Segment Position

Figure 15. (a) Arithmetic sum, divided by two, of observed normal and reverse polarity signal from Figures 11b and 11c, which shows recovery of the relative magnitude of the induced component of magnetization. Note that greater induced magnetization appears toward segment ends and is skewed toward southern (IC) ends of segments. (b) Arithmetic difference, divided by two, of the observed normal and reverse polarity signals from Figures 11b and 11c, which shows recovery of the relative magnitude of the remanent component of magnetization. Note the relatively symmetrical pattern of reduced remanence toward segment ends.

spreading segment, the extrusive layer is probably relatively thin (< 1 km), highly porous, strongly faulted, and continuously permeated by seawater over its full variation in thickness. Thus alteration of the extrusives is most likely similar across an entire segment, and we expect no significant differences between IC, OC, and segment-center extrusive crust.

The observations in this section suggest that magnetization in the extrusive layer may not contribute a significant proportion of the off-axis magnetic anomaly signal. This is consistent with, and buttressed by, our observations that (1) there is an initial rapid decay in magnetization with age, (2) a strong on-axis signal of north-to-south asymmetry in crustal magnetization does not appear to be transported off-axis, and (3) there is a significant difference in the correlation of RMBA gravity versus magnetization on-axis and off-axis. Thus we suggest that much of the along-isochron variation in remanence demonstrated by Figure 15b arises from a deeper source.

If we assume that lower crust (e.g., the gabbros) is the primary carrier of off-axis remanent magnetization, then we can better

explain our observations. Faults reaching to some given depth are more likely to penetrate through a thin layer 2 at the ends of segments and deep into the lower crust, allowing fluid flow and alteration of gabbros. The alteration would reduce the remanent magnetization and might also enhance induced magnetization if the gabbros are serpentinized. Such alteration may be the dominant cause of reduced remanent magnetization in OC ends of segments, whereas at IC ends, thin crust will also contribute to the reduced magnetization. On average, the resulting reduction in remanence is similar for both OC and IC ends (Figure 15b). In thick crust at segment centers, faults reaching to the same subbottom depth as those at segment ends would not affect the lower crust as significantly. Thus segment-center gabbros should be less altered and would retain more of their remanent magnetization.

At both OC and IC segment ends, the effects of faulting and alteration need not be limited to lower crust. Mantle peridotites may also be altered if the crust is thin enough, and serpentinites could contribute significantly to the induced magnetization at segment ends. This effect probably is strongest in the very thin crust at IC ends of segments. We suggest that it explains our observations of enhanced induced magnetization at inside corners (Figure 15a) and the correlation of more positive magnetization with increasing RMBA gravity (thinning crust) (Figure 13).

On the basis of the above observations and interpretations, we speculate that at slow-spreading ridges a major proportion of the off-axis magnetic signal (remanent plus induced magnetization) is carried in the deep crust (i.e., the gabbro section) and to some extent in the uppermost mantle. Evidence that gabbros can sustain a primary remanent magnetization presently is quite limited [*Kent et al.*, 1978; *Dunlop and Prevot*, 1982; *Harrison*, 1987; *Pariso and Johnson*, 1993 a, b; *Xu et al.*, 1997], but the common exposure of these rocks in IC tectonic settings of slow-spreading ridges offers excellent opportunities to further sample and measure the magnetization of the lower crust.

7. Conclusions

From analysis of the magnetization of ocean crust created at the slow-spreading Mid-Atlantic Ridge between 25° and 27°N, we conclude the following:

1. Magnetization shows an initial rapid decay followed by a slower long-term decay (Figure 7). The slow-spreading rate and poor sea-surface resolution of the magnetic anomaly signal does not allow unambiguous resolution of rates of either short-term or long-term decay in magnetization with age. Initial rapid decay certainly occurs within the first few million years, and it may occur in significantly less time. This result is consistent with numerous studies which have shown that young extrusive lavas are initially highly magnetized and that they most likely contribute a major proportion of crustal magnetization at the ridge axis [e.g., *Talwani et al.*, 1971; *Johnson and Atwater*, 1977; *Harrison*, 1987; *Tivey*, 1996], although rapid decay of magnetization with age quickly reduces magnetic anomaly amplitude from the spreading axis to the bounding rift-valley walls [*Johnson and Atwater*, 1977; *Macdonald*, 1977; *Hussenoeder et al.*, 1996]. Once this rapid, large-amplitude magnetization decay has occurred, the remaining magnetic signal appears to decay much more slowly with age.

2. Crustal magnetization at the spreading axis shows a marked along-axis asymmetry, with the southern ends of ridge segments more magnetic than the northern ends (Figure 8). The cause of

this asymmetry is unknown, and there are no known correlative trends in geochemistry [e.g., *Melson and O'Hearn*, 1986] that might explain the change. This distinctive pattern clearly is not translated off-axis in reverse polarity crust, and it is only weakly maintained, if at all, in off-axis normal polarity crust (Figures 9-11). We suggest that the asymmetric pattern of axial magnetization is contained largely in the extrusive crust and that this signal is rapidly attenuated off-axis. This observation is consistent with our first observation of initial rapid decay in crustal magnetization and suggests that the contribution of the extrusives to the magnetic anomaly signal is reduced substantially off-axis.

3. A comparison of RMBA gravity and magnetization suggests no significant correlation between apparent crustal thickness and crustal magnetization along the rift axis. However, a statistically significant correlation is found off-axis. Increased RMBA gravity correlates with more positive magnetization off-axis, regardless of polarity, suggesting an increased component of induced magnetization in thinner crust.

4. Off-axis, segment ends show shifts toward more positive magnetization regardless of initial polarity, which indicates the presence of induced magnetization (Figure 15a). Induced magnetization is prevalent at both OC and IC segment ends but is skewed to higher values at IC ends (Figure 15a). The induced magnetization indicates that crustal alteration is common at segment ends where we expect thinner crust, consistent with the correlation between RMBA gravity and magnetization. We attribute the increased induced magnetization in thin-crust, IC settings, to enhanced serpentinization in near-seafloor mantle peridotites.

5. Remanent magnetization is reduced at segment ends off-axis (Figure 15b). The original remanence is not completely destroyed because a recognizable polarity signal is maintained very close to segment boundaries. There is no consistent difference in the reduction of remanent magnetization between IC and OC ends of segments (Figure 15b), even though RMBA gravity suggests that they have very different crustal thickness. Thus remanent magnetization appears to be independent of crustal thickness and bulk crustal composition off-axis, suggesting that the off-axis thickness or presence of extrusives is not important. We suggest that decreased remanent magnetization at OC ends is primarily due to alteration of the lower crust, but a similar decrease in remanent magnetization at IC ends may be a combination of crustal thinning and alteration.

From these observations, we propose that as extrusive crust is transported off-axis, it rapidly loses the strong magnetization that dominates the axial crustal magnetic signal. Within a few million years, the extrusive crust is no longer the primary contributor to the magnetic-anomaly signal, and another source of magnetic remanence is required to maintain the remanent polarity-reversal pattern and the observed along-isochron variations in magnetization. We suggest the dominant source of this off-axis remanent magnetization is the lower crust, in all likelihood the gabbro section. Partial loss of this remanent magnetization occurs at segment ends through crustal thinning and alteration. Coincident development of induced magnetization in serpentinized gabbros and peridotites at segment ends significantly enhances positive magnetization in both normal and reverse polarity crust.

References

Arkani-Hamed, J., Remanent magnetization of the oceanic upper mantle, *Geophys. Res. Lett., 15*, 48-51, 1988.

Arkani-Hamed, J., Thermoviscous remanent magnetization of oceanic lithosphere inferred from its thermal evolution, *J. Geophys. Res., 94*, 17,421-17,436, 1989.

Bleil, U., and N. Peterson, Variations in magnetization intensity and low-temperature titanomagnetite oxidation of ocean floor basalts, *Nature, 301*, 384-388, 1983.

Cande, S.C., and D.V. Kent, Revised calibration of the geomagnetic polarity timescale for the late Cretaceous and Cenozoic, *J. Geophys. Res., 100*, 6093-6095, 1995.

Cannat, M., Emplacement of mantle rocks in the seafloor at mid-ocean ridges, *J. Geophys. Res., 98*, 4163-4172, 1993.

Cannat, M., et al., Thin crust, ultramafic exposures, and rugged faulting patterns at the Mid-Atlantic Ridge (22-24°N), *Geology, 23*, 49-52, 1995.

Carbotte, S., S. Welch, and K.C. Macdonald, Spreading rates, rift propagation and fracture zone offset histories during the past 5 My on the Mid-Atlantic ridge: 25°-27°30'S and 31°- 34°30'S, *Mar. Geophys. Res., 13*, 51-80, 1991.

Collette, B.J., and W.R. Roest, Further investigations of the North Atlantic between 10° and 40°N and an analysis of spreading from 118 Ma ago to present, *Proc. K. Ned. Akad. Wet., 95*, 159-206, 1992.

Collette, B.J., K. Rutten, H. Schouten, and A.P. Slootweg, Structure of the Mid-Atlantic Ridge Province between 12°N and 18°N, *Mar. Geophys. Res., 2*, 143-179, 1974.

Dick, H., W.B. Bryan, and G. Thompson, Low angle faulting and steady-state emplacement of plutonic rocks at ridge transform intersections, *Eos Trans. AGU, 62*, 406, 1981.

Dunlop, D.J., Theory of the magnetic viscosity of lunar and terrestrial rocks, *Rev. Geophysics, 11*, 855-901, 1973.

Dunlop, D.J., and M. Prevot, Magnetic properties and opaque mineralogy of drilled submarine intrusive rocks, *Geophys. J., 16*, 763-802, 1982.

Escartin, J., and J. Lin, Ridge offsets, normal faulting, and gravity anomalies of slow spreading ridges, *J. Geophys. Res., 100*, 6163-6177, 1995.

Gee, J., and D.V. Kent, Variations in layer 2A thickness and the origin of the central anomaly magnetic high, *Geophys. Res. Lett., 21*, 297-300, 1994.

Grindlay, N.R., P.J. Fox, and P.R. Vogt, Morphology and tectonics of the Mid-Atlantic Ridge (25°-27°30'S) from Sea Beam and magnetic data, *J. Geophys. Res., 97*, 6983-7010, 1992.

Harrison, C.G.A., Marine magnetic anomalies: The origin of the stripes, *Annu. Rev. Earth Planet. Sci., 15*, 505-543, 1987.

Hussenoeder, S.A., M.A. Tivey, H. Schouten, and R. Searle, Near-bottom magnetic survey of the Mid-Atlantic Ridge axis, 24°-24°40'N: Implications for crustal accretion at slow spreading ridges, *J. Geophys. Res., 101*, 22,051-22,069, 1996.

International Association of Geomagnetism and Aeronomy (IAGA), Division V, Working Group 8, International geomagnetic reference field, 1995 revision, *Geophys. J. Int., 125*, 318-321, 1996.

Irving, E., The mid-Atlantic ridge at 45°N, XIV, Oxidation and magnetic properties of basalt; Review and discussion, *Can. J. Earth Sci., 7*, 1528-1538, 1970.

Johnson, H.P., and T., Atwater, Magnetic study of basalts from the Mid-Atlantic ridge, lat. 37°N, *Geol. Soc. Am. Bull., 88*, 637-647, 1977.

Johnson, H.P., and J.E. Pariso, Variations in oceanic crustal magnetization: Systematic changes in the last 160 million years, *J. Geophys. Res., 98*, 435-446, 1993.

Johnson, H.P., and M.A. Tivey, Magnetic properties of zero-age oceanic crust: A new submarine lava flow on the Juan de Fuca Ridge, *Geophys. Res. Lett., 22*, 175-178, 1995.

Karson, J.A., Seafloor spreading on the Mid-Atlantic Ridge: Implications for the structure of ophiolites and oceanic lithosphere produced in slow-spreading environments, in *Proceedings of the Symposium*

TROODOS 1987, edited by J. Malpas, E.M. Moores, A. Panayiotou and C. Xenophontos, pp. 547-555, Geological Survey Dept., Min. of Agriculture and Natural Resources, Nicosia, Cyprus, 1990.

Kent, D.V., B.M. Honnorez, N.D. Opdyke, and P.J. Fox, Magnetic properties of dredged oceanic gabbros and the source of marine magnetic anomalies, *Geophys. J. R. Astron. Soc.*, *55*, 513-537, 1978.

Kleinrock, M.C., B.E. Tucholke, J. Lin, and M.A. Tivey, Fast rift propagation at a slow spreading ridge: Progressive tearing of an entire spreading segment, *Geology*, *25*, 639-642, 1997.

Kuo, B.Y., and D.W. Forsyth, Gravity anomalies of the ridge transform system in the South Atlantic between 31° and 34.5°S: Upwelling centers and variations in crustal thickness, *Mar. Geophys. Res.*, *10*, 205-232, 1988.

Lin, J., G.M. Purdy, H. Schouten, J.-C. Sempéré, and C. Zervas, Evidence for focused magmatic accretion along the Mid-Atlantic Ridge, *Nature*, *344*, 627-632, 1990.

Macdonald, K.C., Near-bottom magnetic anomalies, asymmetric spreading, oblique spreading, and tectonics of the Mid-Atlantic Ridge near lat. 37°N, *Geol. Soc. Am. Bull.*, *88*, 541-555, 1977.

Macdonald, K.C., Mid-ocean ridges: Fine scale tectonic, volcanic and hydrothermal processes within the plate boundary zone, *Annu. Rev. Earth Planet. Sci.*, *10*, 155-190, 1982.

Macdonald, K.C., The crest of the Mid-Atlantic Ridge: Models for crustal generation processes and tectonics, in *DNAG*, vol. M, *The Western North Atlantic Region*, edited by P.R. Vogt and B.E. Tucholke, pp. 51-68, Geol. Soc. of Am., Boulder, Colo., 1986.

Macdonald, K.C., S.P. Miller, S.P. Heustis, and F.N. Spiess, Three-dimensional modelling of a magnetic reversal boundary from inversion of deep-tow measurements, *J. Geophys. Res.*, *85*, 3670-3680, 1980.

Macdonald, K.C., P.J. Fox, L.J. Perram, M.F. Elsen, R.M. Haymon, S.P. Miller, S.M. Carbotte, M.-H. Cormier, and A.N. Shor, A new view of the mid-ocean ridge from the behavior of ridge axis discontinuities, *Nature*, *335*, 217-225, 1988.

McNab, R., J. Verhoef, W. Roest, and J. Arkani-Hamed, New database documents the magnetic character of the Arctic and North Atlantic, *Eos Trans. AGU*, *76*, 449, 1995.

Melson, W.G., and T. O'Hearn, "Zero-age" variations in the composition of abyssal volcanic rocks along the axial zone of the Mid-Atlantic Ridge, in *DNAG*, vol. M, *The Western North Atlantic Region*, edited by P.R. Vogt and B. E. Tucholke, pp. 117-136, Geol. Soc. of Am., Boulder, Colo., 1986.

Pariso, J.E., and H.P. Johnson, Do lower crustal rocks record reversals of the Earth's magnetic field? Magnetic petrology of oceanic gabbros at Ocean Drilling Program Hole 735B, *J. Geophys. Res.*, *98*, 16,013-16,032, 1993a.

Pariso, J.E., and H.P. Johnson, Do Layer 3 rocks make a significant contribution to marine magnetic anomalies? In situ magnetization of gabbros at Ocean Drilling Program Hole 735B, *J. Geophys. Res.*, *98*, 16,033-16,052, 1993b.

Pariso, J.E., C. Rommevaux, and J.-C. Sempéré, Three-dimensional inversion of marine magnetic anomalies: implications for crustal accretion along the Mid-Atlantic Ridge (28°-31°31'N), *Mar. Geophys. Res.*, *18*, 85-101, 1996.

Parker, R.L., and S.P. Huestis, The inversion of magnetic anomalies in the presence of topography, *J. Geophys. Res.*, *79*, 1587-1593, 1974.

Pockalny, R.A., A. Smith, and P. Gente, Spatial and temporal variability of crustal magnetization of a slowly spreading ridge: Mid-Atlantic Ridge (20°-24°N), *Mar. Geophys. Res.*, *17*, 301-320, 1995.

Purdy, G.M., J-C Sempéré, H. Schouten, D.L. Dubois, and R. Goldsmith, Bathymetry of the Mid-Atlantic Ridge, 24°-31°N: A Map series, *Mar. Geophys. Res.*, *12*, 247-252, 1990.

Schouten, H., and C.R. Denham, Modeling the oceanic magnetic source layer, in *Deep Drilling Results in the Atlantic Ocean: Ocean Crust Maurice Ewing Ser.*, vol. 2, edited by M. Talwani, C.G.A. Harrison, and D.E. Hayes, pp. 151-159, AGU, Washington, D. C., 1979.

Sempéré, J.-C., High magnetization zones near spreading center discontinuities, *Earth Planet. Sci. Lett.*, *107*, 389-405, 1991.

Sempéré, J.-C., K.C. Macdonald, and S. Miller, Overlapping spreading centers: 3-D inversion of the magnetic field at 9°30'N in the East Pacific Rise, *Geophys. J. R. Astron. Soc.*, *79*, 799-812, 1984.

Sempéré, J.-C., J. Lin, H.S. Brown, H. Schouten, and G.M. Purdy, Segmentation and morphotectonic variations along a slow-spreading center: The Mid-Atlantic Ridge (24°00'N - 30°40'N), *Mar. Geophys. Res.*, *15*, 153-200, 1993.

Sinha, M.C., and K.E. Louden, The Oceanographer Fracture Zone, I, Crustal structure from seismic refraction studies, *Geophys. J.*, *75*, 713-716, 1983.

Sinton, J.M., and R.S. Detrick, Mid-ocean ridge magma chambers, *J. Geophys. Res.*, *97*, 197-216, 1992.

Sloan, H., and P. Patriat, Kinematics of the North American-African plate boundary between 28° and 29°N during the last 10 Ma: Evolution of the axial geometry and spreading rate and direction, *Earth Planet. Sci. Lett.*, *113*, 323-341, 1992.

Smith, D.K., and J. Cann, The role of seamount volcanism in crustal construction at the Mid-Atlantic Ridge (24°-30°N), *J. Geophys. Res.*, *97*, 1645-1658, 1992.

Smith, W.H.F., and P. Wessel, Gridding with continuous curvature splines in tension, *Geophysics*, *55*, 293-305, 1990.

Talwani, M., C.C. Windisch, and M.G. Langseth, Reykjanes ridge crest: a detailed geophysical study, *J. Geophys. Res.*, *76*, 473-517, 1971.

Tivey, M.A., The vertical magnetic structure of oceanic crust determined from near-bottom magnetic field measurements, *J. Geophys. Res.*, *101*, 20,275-20,296, 1996.

Tivey, M.A., and H.P. Johnson, The characterization of viscous remanent magnetization in large and small magnetite particles, *J. Geophys. Res.*, *89*, 543-552, 1984.

Tivey, M.A., and H.P. Johnson, Alvin magnetic survey of zero-age crust: Coaxial segment eruption, Juan de Fuca Ridge 1993, *Geophys. Res. Lett.*, *22*, 171-174, 1995.

Tolstoy, M., A.J. Harding and J.A. Orcutt, Crustal thickness on the Mid-Atlantic Ridge: Bull's-eye gravity anomalies and focused accretion, *Science*, *262*, 726-729, 1993.

Tucholke, B.E., and J. Lin, A geological model for the structure of ridge segments in slow-spreading crust, *J. Geophys. Res.*, *99*, 11,937-11,958, 1994.

Tucholke B.E. and H. Schouten, Kane fracture zone, *Mar. Geophys. Res.*, *10*, 1-39, 1988.

Tucholke, B.E., J. Lin, M.C. Kleinrock, M.A. Tivey, T. Reed, J. Goff, and G.E. Jaroslow, Segmentation and crustal structure of the western Mid-Atlantic Ridge flank, 25°30'-27°10' and 0-29 M.Y., *J. Geophys. Res.*, *102*, 10,203-10,244, 1997.

Vine, F.J., Spreading of the ocean floor: New evidence, *Science*, *154*, 1405-1415, 1966.

Vine, F.J., and D.H. Matthews, Magnetic anomalies over oceanic ridges, *Nature*, *199*, 947-949, 1963.

Vogt, P.R., Magnetic anomalies and crustal magnetization, in *DNAG*, vol. M, *The Western North Atlantic Region*, edited by P.R. Vogt and B.E. Tucholke, pp. 229-256, Geol. Soc. of Am., Boulder, Colo., 1986.

Vogt, P.R., and G.L. Johnson, Magnetic telechemistry of oceanic crust?, *Nature*, *245*, 373-375, 1973.

Weiland, C., K.C. Macdonald, and N. Grindlay, Ridge segmentation and the magnetic structure of the Southern Mid-Atlantic ridge 26°S and 31°-35°S: Implications for magmatic processes at slow spreading centers, *J. Geophys. Res.*, *101*, 8055-8073, 1996.

Wittpenn, N.A., C.G.A. Harrison, and D.W. Handschumacher, Crustal magnetization in the South Atlantic from inversion of magnetic anomalies, *J. Geophys. Res.*, *94*, 15,463-15,480, 1989.

Xu, W., J.W. Geissman, R. Van de Voo, and D.R. Peacor, Electron microscopy of iron oxides and implications for the origin of magnetizations and rock magnetic properties of Banded Series rocks of the Stillwater Complex, Montana, *J. Geophys. Res.*, *102*, 12,139-12,157, 1997.

M.A. Tivey and B.E. Tucholke, Department of Geology and Geophysics, Woods Hole Oceanographic Institution, Woods Hole, MA 02543-1542. (e-mail: mtivey@whoi.edu; btucholke@whoi.edu)